

## The Solar Neighborhood XXIX: The Habitable Real Estate of our Nearest Stellar Neighbors

Justin R. Cantrell, Todd J. Henry, Russel J. White

*Georgia State University, Atlanta, GA 30302-4106*

cantrell@chara.gsu.edu, thenry@chara.gsu.edu, white@chara.gsu.edu

### ABSTRACT

We use the sample of known stars and brown dwarfs within 5 pc of the Sun, supplemented with AFGK stars within 10 pc, to determine which stellar spectral types provide the most habitable real estate — defined to be locations where liquid water could be present on Earth-like planets. Stellar temperatures and radii are determined by fitting model spectra to spatially resolved broad-band photometric energy distributions for stars in the sample. Using these values, the locations of the habitable zones are calculated using an empirical formula for planetary surface temperature and assuming the condition of liquid water, called here the empirical habitable zone, or EHZ. Systems that have dynamically disruptive companions, assuming a 5:1 separation ratios for primary/secondary pairs and either object and a planet, are considered not habitable. We use the results of these calculations to derive a simple formula to predict the location of the EHZ for main sequence stars based on  $V - K$  color. We consider EHZ widths as more useful measures of the habitable real estate around stars than areas because multiple planets are not expected to orbit stars at identical stellar distances. This EHZ provides a qualitative guide on where to expect the largest population of planets in the habitable zone of main sequence stars. Because of their large numbers and lower frequency of short-period companions, M stars provide more EHZ real estate than other spectral types, possessing 36.5% of the habitable real estate *en masse*. K stars are second with 21.5%, while A, F, and G stars offer 18.5%, 6.9% and 16.6%, respectively. Our calculations show that three M dwarfs within 10 pc harbor planets in their EHZs — GJ 581 may have two planets (d with  $m \sin i = 6.1 M_{\oplus}$ ; g with  $m \sin i = 3.1 M_{\oplus}$ ), GJ 667 C has one (c with  $m \sin i = 4.5 M_{\oplus}$ ), and GJ 876 has two (b with  $m \sin i = 1.89 M_{Jup}$  and c with  $m \sin i = 0.56 M_{Jup}$ ). If Earth-like planets are as common around low mass

stars as recent Kepler results suggest, M stars are the most likely place to find Earth-like planets in habitable zones.

*Subject headings:* stars: habitable zones – solar neighborhood

## 1. Introduction

Early astronomers looked to the sky and saw the Moon as a habitable world covered in vast oceans, Venus as a swampy marshland enshrouded in clouds, and Mars with grand canals (Lowell 1895). Not one of these worlds has maintained its promise of abundant life. Instead, the Solar System, once thought to be teeming with life, may be barren, although hope remains for environments under the icy crust of Europa (Marion et al. 2003), in the tiger stripes of Enceladus (Parkinson et al. 2007), in water under the Martian surface (Malin & Edgett 2000), or perhaps lurking somewhere as yet unidentified. With the discovery of more than 700<sup>1</sup> extrasolar planets since 1989, the real estate market in our Solar System is no longer the only place we might look for evidence of life beyond Earth. A likely place to search for planets harboring life is in the habitable zones of nearby stars.

The term “habitable zone” was first coined by Huang (1959) as a region around a star where a planet could support life. Since then, there have been many definitions of habitability, most based on the presence of liquid water on the surface of a planet. These planets could be terrestrial in nature, which are known to exist (Borucki & the Kepler Team 2010), or perhaps moons of gas-giant planets, which are suspected to exist (Weidner & Horne 2010). Examples of nearby stars hosting potentially habitable super-Earths include GJ 581, an M dwarf with potentially two planets in its habitable zone (Mayor et al. 2009; Vogt et al. 2010b) and GJ 667C, another M dwarf with one planet in its habitable zone (Anglada-Escudé et al. 2012).

Kasting et al. (1993) did pioneering work in describing habitable zones (HZs) around main sequence stars. To approximate the location of the HZ, they introduced a one-dimensional climate model that yields the distances from main sequence stars where liquid water would be present, given an initial assumption of a  $CO_2/H_2O/N_2$  atmosphere and an Earth-sized planet. They describe the inner boundary of their model as the point at which the atmosphere becomes saturated with  $H_2O$ , causing a loss of water via photolysis and hydrogen escape; the outer boundary is marked by the formation of  $CO_2$  clouds that cool a planet’s surface by increasing its albedo and lowering its convective lapse rate. They give an

---

<sup>1</sup>(May 2013) <http://www.exoplanets.org>

equation for the distance from a star,  $D$ , of the HZ in AU based on the incident flux that a planet receives,  $L/L_{\odot}$ , the star’s luminosity relative to that of the Sun, and  $S_{eff}$ , the ratio of outgoing IR flux to the incoming incident flux at the top of the planet’s atmosphere:

$$D = 1AU \left( \frac{L/L_{\odot}}{S_{eff}} \right) \quad (1)$$

Using more explicit terms, Equation 1 can be used to show the distance from a star at which a planet would have a given temperature, based on energy balance (Kaltenegger et al. 2002). Equation 2 can then be used to show that the equilibrium temperature,  $T_P$ , of a planet at a distance,  $D$ , from its host star is a function of the stellar effective temperature,  $T_{eff}$ , stellar radius,  $R_{\star}$ , and the planet’s Bond albedo,  $A$ . Thus, if the stellar  $T_{eff}$  and  $R_{\star}$  are known, we can calculate the range of distances where a planet with given albedo<sup>2</sup> would have a surface temperature suitable for liquid water, as described by the planet’s temperature,  $T_P$ :

$$T_P = T_{eff} \left( \frac{R_{\star}}{2D} \right)^{1/2} (1 - A)^{1/4} \quad (2)$$

In this paper, we apply this equation to the nearby population of stars whose stellar properties are well known to estimate the total habitable real estate that they provide. We use the complete sample of all stars currently known to be within 5 pc of the Sun from Henry (2012), and an extended 10 pc sample of AFGK stars, as well as binary properties, photometric and astrometric data. We present our derived  $T_{eff}$  and  $R_{\star}$  for each star in the sample and discuss the methods used to derive each star’s empirical habitable zone (EHZ). For multiple star systems, we assess dynamical stability to eliminate stellar systems unsuitable for long-term planetary orbits. Our main goal is to determine, as a function of spectral type, the cumulative available EHZ in the solar neighborhood.

## 2. Motivations for this Study

We do not yet have a detailed understanding of the architectures of all types of planetary systems orbiting various types of stars, although there has been recent progress for planets in close to stars via the Kepler mission (e.g., Howard et al. 2012 for planets in orbital periods less than 50 days around FGKM stars). In this paper we assume no bias in the final locations

---

<sup>2</sup> $A = 0.3$  for the hypothetical planets used in this paper.

of planets around stars, including formation and migration (i.e., we assume the distribution of planets to be uniform in semi-major axis), to assess the integrated EHZs of various types of stars found in the solar neighborhood. We focus on the presence of the *first* habitable planet around a given star, although wider EHZs may of course include more than one planet. This is an important assessment to make given the limited telescope time, funding, and energy of astronomers, so here we focus on the question, “What set of targets might be most appropriate to observe to improve the odds of detecting at least one habitable planet?” This question is posed in wide-ranging arenas, from conversations between students and faculty when developing research projects, to discussions of programmatic directions such as those of NASA’s Exoplanet Program Analysis Group and the NASA/NSF Exoplanet Task Force.

In this paper we evaluate stars within 10 pc in a consistent fashion to assess what spectral types offer the greatest promise for nearby habitable planets. The nearby sample contains stars that have been characterized carefully, and as a population provide the most accurate snapshot of the stellar content of the Galaxy. Thus, this sample provides the foundation for a realistic understanding of the relative merits of examining different types of stars. Our results, coupled with the planet frequency statistics from the Kepler mission, (e.g., Borucki and Koch 2011, Howard et al. 2012, and Dressing and Charbonneau 2013), can provide statistical measures for the of number of habitable planets within larger stellar populations, and particularly among volume-limited samples of nearby stars, as we build to a comprehensive sample of the nearest stars (e.g., Henry et al. 2006; Henry 2012). For example, Howard et al. (2012) show that the number of super-Earth size planets increases with decreasing  $T_{eff}$  for orbital periods less than 50 days. Dressing and Charbonneau (2013) show that for cool stars ( $T_{eff} < 4000\text{K}$ ) the occurrence rate for planets with  $0.5\text{--}4 R_{\oplus}$  is 0.9 planets per star for orbital periods less than 50 days. They also calculate that the lower limit on the occurrence rate of Earth-size planets in the HZ of cool stars is 0.04 with a 95% confidence. Using the population we describe here, this implies that there could be two Earth-size planets within the EHZs of M dwarfs within 5 pc of the Sun. Assuming a constant density of M dwarfs to 10 pc (not all of which have yet been identified) the number of Earth-size planets jumps to 16. One of the primary motivations of this study is to determine, in aggregate, how the odds of finding such planets around M dwarfs compares to other spectral types.

The results of our habitable real estate calculations, as outlined in this paper, are particularly valuable in highlighting that the ubiquitous M dwarfs provide many locales meeting the canonical definition for habitability. Current searches for habitable worlds orbiting the nearest stars have yielded many Jovian planets and a few terrestrial worlds, but most of the searches to date have been carried out using the radial velocity technique and have focused on bright FGK stars that provide many photons to spectrographs (and which are in the

sweet spot for Kepler). For transit searches, M dwarfs provide higher contrast ratios for a given planet, whereas for radial velocity and astrometric searches they provide larger wobbles for a planet than do more massive FGK stars. Knowing that the M dwarfs, as a group, are important stars to search for habitable worlds helps direct our focus back to the solar neighborhood, in which three-quarters of all stars are red dwarfs. Because of their proximity, these stars hold great promise for the detailed characterization of exoplanets.

### 3. Properties of our Nearest Neighbors

Primary science goals of the Research Consortium on Nearby Stars (RECONS<sup>3</sup>) and the Center for High Angular Resolution Astronomy (CHARA<sup>4</sup>), are to find and determine the fundamental properties of our nearest stellar neighbors. This has led to the most complete assessment to date of stars within 5 pc of the Sun.

#### 3.1. The 5 pc Sample

The modern sample of all known stars and brown dwarfs within 5 pc of the Sun (Henry 2010, 2012), listed in Table 1 (assembled photometry in Table 2) was first published in the *Observer's Handbook 2010*. The sample, which is updated yearly, was created using the combination of several ground-based and space-based parallax programs, including the General Catalogue of Trigonometric Stellar Parallaxes (van Altena et al. 1995), Hipparcos (Perryman et al. 1997), RECONS (Henry et al. 1997, 2006; Deacon et al. 2005; Jao et al. 2005; Costa et al. 2005), HST (Benedict et al. 1999, 2002), Gatewood (1989, 1994) and Gatewood et al. (1992, 1993). To be included in the sample, a system must have a weighted mean trigonometric parallax measurement of 200 mas or greater with an error of 10 mas or less. To create this sample the parallaxes compiled were combined and weighted based on the individual measurement errors. The spectral type, with reference, for each star or star system is given with the astrometric data, including RA, Dec, the weighted mean trigonometric parallax, and the number of parallaxes included in the weighted mean, in Table 1. The closing date for the sample is 2012.0.

The 5 pc sample contains 67 stars, including the Sun, and 4 presumed brown dwarfs (spectral types L or T) in 50 systems. Of the 50 systems, 34 are single, 11 are binaries, and

---

<sup>3</sup><http://recons.org>

<sup>4</sup><http://www.chara.gsu.edu/CHARA/>

5 are triples, giving a multiplicity fraction of 32%. This fraction is consistent with previous volume limited surveys (35%; Reid & Gizis 1997). The majority (85%) of the sample are main sequence stars; the exceptions include Procyon (GJ 280A), which has a slightly evolved spectral type of F5IV-V, 5 white dwarfs, and the 4 L/T dwarfs. The spectral type breakdown includes 1 A, 1 F, 3 G’s (including the Sun), 7 K’s, 50 M’s, 1 L, 3 T’s, and 5 white dwarfs. We do not include white dwarfs and brown dwarfs in subsequent calculations of habitable real estate, as they are objects that are cooling continually, resulting in unsustainable HZs on long ( $\sim$ Gyr) timescales.

### 3.2. An Estimated 10 pc Sample

Due to the sparse population of all but the M stars in the 5 pc sample, it is difficult to draw meaningful statistics to estimate which stellar spectral types possess the most habitable real estate. Therefore, we extend our sample to 10 pc for A, F, G and K stars. Using the Hipparcos Catalog, which is complete to  $V=9$  (Perryman et al. 1997), we selected all objects with a parallax greater than 100 mas for inclusion into the sample. We expect that the extended 10 pc sample is complete for spectral types A through K, given  $M_v=9.0$  for a M0.0V star (Henry et al. 2006). However, rather than using spectral type as a selection criterion, we used a color cutoff of  $V - K \leq 3.5$  as the dividing line between K and M dwarfs (Kenyon & Hartmann 1995). As with the 5 pc sample, weighted mean parallaxes from the General Catalogue of Trigonometric Stellar Parallaxes, The Hipparcos Catalog and other sources are listed with the astrometry data for the extended 10 pc sample in Table 3, as well as spectral types and references. Available photometric data are listed in Table 4. We note that there are no O type or B type stars within 10 pc. Because the M star population is not complete out to 10 pc (Henry et al. 2006), we approximate the total M star population by scaling by a factor of eight from the 5 pc sample. For clarity, we refer to the additional AFGK stars from 5-10 pc as the “extended 10 pc sample” and our estimates of all AFGKM stars within 10 pc as the “estimated 10 pc sample”. In total, the stellar population of the estimated 10 pc sample consists of 66 AFGK stars in 57 systems. Broken down by spectral type, the sample contains 4 A stars, 6 F stars, 21 G stars, 35 K stars and an estimated 400 M stars within 10 pc.

### 3.3. Photometry and Energy Distributions

The *UBVRI* photometry used in this paper, listed in Tables 2 & 4, was extracted from sources in the literature with preference given to large surveys and measurements consistent

with photometry obtained as part of the CTIO Parallax (CTIOPI) program, which uses the Johnson-Kron-Cousins system.  $R$  and  $I$  magnitudes from the USNO-B1.0 catalog (Monet et al. 2003) are incorporated in the extended 10 pc sample and both are rounded to the nearest 0.1 mag.  $R$  magnitudes are averaged from the first and second epochs.

The majority of  $JHK$  photometry is taken from the 2MASS database, identified as those values with errors listed explicitly in Tables 2 and 4 (Cutri et al. 2003). In cases of close binaries with magnitude difference measurements in the literature (e.g., Henry & McCarthy 1993 and Henry et al. 1999), the optical and 2MASS photometry is used with the published magnitude differences to split the component fluxes into individual magnitudes. Note that stars brighter than  $\sim 5$  mag are saturated in 2MASS images and typically have relatively large photometric errors ( $\geq 0.2$  mag). Where possible, we use  $JHK$  measurements in the literature for these stars (Johnson et al. 1966; Johnson et al. 1968; Glass 1975; Mould & Hyland 1976). These magnitudes, listed in their unconverted form in Tables 2 & 4 and with specific references listed in the error columns, were then converted to 2MASS magnitudes using color transformations from Carpenter (2001). Of the 16 multiple systems in the 5 pc sample, eight have spatially unresolved photometry in some or all passbands and are marked as “Joint” in the Notes section of Table 2. Similarly, 10 of the 19 multiple systems in the extended 10 pc sample have spatially unresolved photometry in some or all passbands and are listed as “Joint” in the Notes section of Table 4.

#### 4. Methodology to Derive the EHZ

The HZ around a star is primarily a function of the total energy output of a star that reaches the surface of a planet. This can be determined if the stellar temperature and radius are known, which we calculate for our sample of stars as described in Section 4.1. However, a range of other factors, such as atmospheric pressure, composition, and cloud cover play roles in determining the surface temperature of a planet. To account for this, in Section 4.2 we follow previous studies and approximate these effects by using empirical temperature constraints provided by planets in the Solar System.

##### 4.1. SED Fitting used to Derive Stellar Temperature and Radius

Although spectral types are often used to estimate stellar effective temperatures, the various methods for determining spectral types are inhomogeneous and often depend upon the spectral range used. As an alternative, we fit synthetic stellar spectra to broad-band

energy distributions to determine effective temperatures and radii. In particular, we use photometric measurements spanning *UBVRIJHK* (0.3 to 2.4  $\mu\text{m}$ ) in conjunction with model spectra generated using the PHOENIX code (Hauschildt et al. 1999). This prescription is only used for single stars and for stars in multiple systems in the 5 pc and extended 10 pc samples with at least four spatially resolved photometric measurements in different filter bandpasses. Estimates for unresolved multiples are discussed in Section 4.3.

These available models span the temperature ranges of  $T_{eff}$  of 10,000 K to 7000 K in 200 K increments and 6900 K to 2000 K in 100 K increments. The model spectra have a resolution of 2  $\text{\AA}$  and range from 10  $\text{\AA}$  to 500  $\mu\text{m}$ . The models were convolved with *UBVRIJHK* filter responses to create synthetic photometry. For the *UBVRI* synthetic photometry, we took zero points from Bessell et al. (1998) and filter responses from CTIO<sup>5</sup>. *JHK* filter responses and zero points were from 2MASS<sup>6</sup>. The zero points adopted are listed in Table 5. We adopt  $\log g$  values of 4.5 or 5.0 for all stars.

Solar metallicity is adopted for all stars except GJ 191 ( $\text{Fe}/\text{H} = -0.98$ ; Woolf and Wallerstein 2005) and GJ 451 ( $\text{Fe}/\text{H} = -1.16$ ; Valenti and Fisher 2005), for which we adopt metallicities of  $-1.0$ . The assumption of solar metallicity for the remainder of our 10 pc sample is based on the 36 FGK stars that overlap with Valenti and Fisher (2005). These stars have an average metallicity of  $\text{Fe}/\text{H} = -0.048$  with a standard deviation of 0.168 dex.

The flux values in the model spectra are given as a surface flux that must be scaled by a radius to a known distance for fitting with observed integrated flux values. A stellar radius grid from 0.001  $R_{\odot}$  to 3.00  $R_{\odot}$  with a step size of 0.001  $R_{\odot}$  is calculated for each model spectrum. Each spectrum and radius combination is then convolved with filter response and the zero point data referenced above to derive consequent fluxes observed at Earth. These integrated fluxes are then fit via a  $\chi^2$  minimization routine, written in IDL and described in Equation 3, to compare the model flux with the observed flux across each filter bandpass. Here,  $O$  is the observed integrated flux from the photometric measurements,  $E$  is the estimated integrated flux from the model grids,  $\nu$  is the number of photometric points (degrees of freedom), and  $\sigma$  is the average error in the photometric measurement. Examples of fits for AFGKM stars in the 5 pc sample are shown in Figure 1.

$$\chi_{\text{red}}^2 = \frac{\chi^2}{\nu} = \frac{1}{\nu} \sum \frac{(O - E)^2}{\sigma^2} \quad (3)$$

---

<sup>5</sup><http://www.ctio.noao.edu/instruments/filters/>

<sup>6</sup><http://www.ipac.caltech.edu/2mass/releases/allsky/doc/>



The output is an effective temperature from the model and a radius that best fits the measured photometric data. We assume no interstellar extinction for our sample, and choose four photometric points as the minimum number needed to make a fit. When deriving radii, all stars in the sample are assumed to be spherical and radiate isotropically, which is not the case for rapidly rotating stars that may be oblate and experience gravity darkening (e.g., Altair, see Monnier et al. 2007; Vega, see Aufdenberg et al. 2006). This is most common among stars earlier than mid-F spectral type, as these stars are fully radiative and consequently do not possess an efficient rotational braking mechanism (e.g., Wilson 1965). However, all but one early type star (i.e., earlier than spectral type F5) within 10 pc have projected rotational velocities less than 100 km/s, which correspond to projected oblateness values  $\lesssim 2\%$  (Absil et al. 2008). These apparently slow rotating stars include Sirius A (GJ 244, A1V, 16 km/s; Royer 2002), Procyon A (GJ 280, F5V-IV, 4.9 km/s; Fekel 1997), Vega (GJ 721, A0V, 24 km/s; Royer 2007), and Fomalhaut (GJ 881, A4V, 93 km/s; Royer et al. 2007). We note that despite having a small  $v \sin i$  value, Vega is believed to be rapidly rotating with a nearly pole on orientation (Aufdenberg et al. 2006). An additional rapidly rotating star is Altair (GJ 768, A7V, 217 km/s; Royer 2007) which has an oblateness of 18% determined from interferometric measurements by the CHARA Array (Monnier et al. 2007). As expected, our derived radii and effective temperatures for Altair and Vega are intermediate to the polar and equatorial values listed in Monnier et al. (2007) and Aufdenberg et al. (2006), respectively. Because the EHZ boundaries are a function of the square root of the total luminosity (see Section 4.2), our adopted methodology should yield reliable estimates of the habitable real estate these stars provide, even if the stellar temperatures vary with stellar latitude.

As a consequence of the limited temperature resolution of the PHOENIX grids used ( $\Delta T=200\text{K}$  from 10000K to 7000K and  $\Delta T=100\text{K}$  from 6900K to 2000K), the fitting routine can determine a slightly larger radius coupled with a cooler temperature, or vice versa. Systematic uncertainties in the PHOENIX models are such that a  $\Delta T$  of less than 100K are unreliable (Hauschildt, priv. comm.). As the Stefan-Boltzmann law shows  $R_{\star}^2 T_{eff}^4 \sim L_{\star}$ , the luminosity determined from the SED remains the same as long as the radii and effective temperatures move in opposite directions, and therefore the EHZ, being a function of the square root of the luminosity, does not change. Of key importance, the output radii and temperatures determined here allow us to compare our results directly to those found via interferometric techniques.

Of the stars investigated, 28 have spatially resolved angular diameters from long baseline interferometric instruments such as CHARA, PTI, and VLTI (Table 6). Fifteen of these measurements are from the recent effort of Boyajian et al. (2012). Because these measurements determine sizes to within a few percent, we use them to test the accuracy of the

radii determined in our fitting process. The published radii are on average 7.4% larger than our derived radii, which shows a systematic effect. Our derived model  $T_{eff}$  are on average 2.4% hotter than derived from interferometric measurements. A comparison of our model versus published values is shown in Figure 2. The temperature uncertainties correspond to spectral type uncertainties of 1-2 spectral subclasses, similar to the error associated with most spectral classification methods. As the average values indicate, the overprediction of temperature leads to the expected under-prediction of radius, and the combination yields a more accurate luminosity, and thus consistent EHZ. Given this agreement, we adopt our model values for  $T_{eff}$  and  $R/R_{\odot}$  in final calculations of the habitable real estate.

A few stars are worthy of note. Procyon is slightly evolved (F5.0IV-V) and has a highly constrained  $\log g$  of  $4.05 \pm 0.04$  (Fuhrmann et al. 1997) measured via high resolution spectroscopy in concert with masses determined using astrometry from the Procyon-white dwarf orbit. We adjusted the  $\log g$  to 4.0 for this star and recomputed the  $T_{eff}$  and  $R$ . This, nevertheless, yielded identical values within the model grid resolution as those of  $\log g=4.5$ . The model spectra used in this work have a low temperature limit of 2000 K, which is the value derived for the three intrinsically faintest stars in this sample: SCR 1845-6357A (M8.5V), DEN 1048-3956 (M8.5V), and LP 944-020 (M9.0V).

## 4.2. Habitable Zones of Single Stars

Kasting et al. (1993) use a one-dimensional climate model to calculate HZs around single main sequence stars. A one-dimensional climate model characterizes a planet’s global temperature by dividing the planet into latitudinal bands, and treats the planet as uniform with respect to longitude. These one-dimensional radiative-convective models are a good approximation of global temperature, but more complicated 3-D global climate models are needed to account for the complex physical interactions associated with oceans, clouds, and land surface processes. These inputs add parameters such as land/ocean surface coverage and clouds, which can vary from planet to planet, complicating the overall goal to characterize the EHZ of a star. Here we use the one-dimensional model to generalize the EHZ, and adopt a modified version of the one-dimensional model based on the “Venus and early Mars criterion” from Selsis et al. (2007). In that work, they argue that empirical evidence shows that Venus has not had water on its surface for at least one billion years, and Mars had water on its surface around 4 billion years ago. The solar fluxes at those times were 8% and 28% lower, respectively (Baraffe et al. 1998). Venus (0.72 AU today) and Mars (1.52 AU today) would need to be at distances of  $\sim 0.75$  AU and  $\sim 1.77$  AU, respectively, to receive these levels of solar flux today.

Selsis et al. (2007) provide a method for estimating the inner and outer edges of HZs for stars with  $T_{eff} = 3700\text{K}-7200\text{K}$ . The stars in the sample discussed here range in temperatures from 2000K to 10000K. We have therefore chosen to derive new relations for the HZ boundaries that span the entire stellar temperature regime of our sample, and thereby provide a consistent methodology for all stars in the sample.

In defining our EHZ inner and outer boundaries, we assume a planet with an atmosphere, radius, mass, and Bond albedo (0.3) that matches Earth (Kasting 1996). This leads to the EHZ Equations 4 and 5, used to determine the empirical surface temperature of an Earth-like planet that satisfies the “Venus criterion” (we adopt 0.80 AU on the suggestion of Kasting, priv. comm.) and “Mars criterion” (1.77 AU). The resulting inner and outer radii of the EHZ correspond to equilibrium temperatures of 285 K to 195 K, respectively.

$$R_{EHZinner} = \frac{R_{\star}}{2}(0.7)^{1/2} \left( \frac{T_{eff}}{285K} \right)^2 \quad (4)$$

$$R_{EHZouter} = \frac{R_{\star}}{2}(0.7)^{1/2} \left( \frac{T_{eff}}{195K} \right)^2 \quad (5)$$

Note that these only depend on  $R_{\star}$  and  $T_{eff}^2$ , or essentially the square root of the star’s luminosity. Values for both samples are listed in Tables 7 and 8. Only stars used in the cumulative EHZ calculations are listed, except for the cases of Sirius (GJ 244A) and Procyon (GJ 280A), which provide useful benchmarks.

### 4.3. Habitable Zones of Multiple Star Systems

Although stars in multiple systems are often avoided in planet searches, planets have been found in binary and multiple systems (e.g. Patience et al 2002; Raghavan et al. 2006; Eggenberger et al. 2007). The potentially dynamically disruptive effects of any close stellar companion must be considered when assessing the possibility of formation, long-term dynamical stability, and ultimately the habitability of planets in multiple star systems. The  $\alpha$  Centauri triple system, at a distance from the Sun of 1.34 pc for the G2V-K0V pair (GJ 559 AB) and 1.30 pc for the wide M5V companion (GJ 551), includes the nearest set of Sun-like stars, and provides a test case to study the habitability of multiple stars. The G-K pair has an orbit with a semimajor axis of  $17''.57$  and eccentricity of 0.518 (Pourbaix et al. 2002). This gives periastron and apastron distances of 11.33 AU and 26.67 AU, respectively. Barbieri et al. (2002) show for  $\alpha$  Centauri A that planets can form in stable orbits on a timescale of 5 Myr. Using numerical simulations, they show that not only could planets form, but in

some models they formed directly in the habitable zone. Quintana et al. (2007) similarly find that binary separations greater than 10 AU did not inhibit the formation of terrestrial planets at 2 AU. Consistent with this, Wiegert & Holman (1997) show that the orbit of a planet can be stable as long as the ratio of the semimajor axis of the binary to that of the planet is more than 5:1.

The 36 multiple systems in the 5 pc and extended 10 pc samples consist of 27 binaries, 6 triples, and 3 quadruple systems (GJ 423, GJ 570, and GJ 695), for a total of 84 stars/brown dwarfs. However, nine are not main sequence stars, and excluded because of their evolutionary states (e.g., sub-giants, white dwarfs, and brown dwarfs). Additionally, 16 are M star companions in the extended 10 pc AFGK sample. Because the habitable real estate of M stars out to 10 pc is estimated by scaling the 5 pc results, we do not consider these M stars in our EHZ calculations. This leaves 59 stars in multiple systems with potential habitable zones. For clarity, we emphasize that the EHZ of each star in a system is calculated separately.

Of the 59 stars, 43 (73%) have at least 4 spatially resolved photometric measurements in different filter bandpasses. For these stars, the same prescription used in Section 4.2 is used to calculate the EHZs. For the 16 stars that are not photometrically spatially resolved from their nearest companion(s), we estimate the EHZ locations based on spectral type information for the components. Using the assembled spectral types listed in Tables 1 & 3, we estimate the components'  $V - K$  color using the spectral type versus  $V - K$  colors relations of Kenyon & Hartmann (1995), and estimate the location of the EHZs using the relations described in Section 5.2.

To assess the dynamical stability of any planets in these EHZs, we compare the locations of the outer EHZ boundaries to the binary separations listed in Table 9. We consider a planet to be dynamically stable if the periastron distance of a star's nearest companion is greater than five times the outer EHZ boundary. In cases where the periastron distance can not be calculated (because its full orbit solution is not known), we use the projected separation. Fortunately, these exceptions are all large separation multiples, and thus minor errors in the adopted separation are likely irrelevant for dynamical stability considerations. The ratios of periastron distances to outer EHZ boundaries are illustrated in Figure 3. For each star and its nearest companion, the ratios range from 0.001 to 164107. 49 of the 59 stars have ratios greater than 5 to their nearest companions, and thus EHZs in which planets should be in dynamically stable orbits. The remaining 10 stars (GJ 53A, GJ 222A, GJ 244A, GJ 280A, GJ 423A, GJ 423B, GJ 713A, GJ 713B, GJ 866A, and GJ 866C) are considered to have EHZs in which planets would not be in dynamically stable orbits, so are excluded in our estimate of total EHZ real estate. Seven of these have ratios less than 1.0, hinting at

the possibility of circumbinary planets. However, the majority of the EHZ outer radii are only a few times the binary separations, making it unlikely that these systems would have dynamically stable circumbinary planets in the EHZ. Nonetheless, it is worth noting that a few massive planets have been reported in circumbinary orbits (Lee et al. 2009; Qian et al 2010).

## 5. Discussion

The described HZ calculations are used to assess the total habitable real estate in the solar neighborhood and to determine the amount of habitable real estate as a function of spectral type. Evolved stars, brown dwarfs, and multiple stars with separations detrimental to the orbital stability of a planet in the EHZ, as described above, are excluded in these assessments. In the 5 pc sample, stars removed from the analysis due to close companions include GJ 244A, GJ 244B, GJ 280A, GJ 280B, GJ 866A, and GJ 866C. The distribution by spectral type, after the removal of these stars in the 5 pc sample is as follows: 0 A, 0 F, 3 G, 7 K, and 48 M stars. Similarly, stars removed from the extended 10 pc sample analysis due to close companions include GJ 53A, GJ 53B, GJ 222A, GJ 222B, GJ 423A, GJ 423 B, GJ 423C, GJ 423D, GJ 713A, and GJ 713B. Stars with evolved spectral types such as GJ 150, GJ 695A, and GJ 780 are also removed from subsequent calculations. By spectral type, the total stellar samples considered in the final EHZ assessment are 3 A, 4 F, 14 G, 34 K, and an estimated 384 M stars.

### 5.1. The EHZ “Width”

Using our initial assumptions of a terrestrial “Earth-like” planet as the basis for our EHZ, we estimate the habitable real estate using linear AU separations from the central star, essentially the width of the EHZ. In Table 10 we present the EHZ width totals for each spectral type in the 5 pc and total 10 pc samples.

The cumulative EHZ width for stars in the 5 pc subsample is 8.8 AU, including 2.6 AU for the 3 G stars (including the Sun) and 2.9 AU for the 7 K stars. The 48 M dwarfs in the 5 pc sample *en masse* provide 3.3 linear AU available for habitable planets, or 38% of the available EHZ. The dominant contribution of M dwarfs to the EHZ width is demonstrated clearly using the estimated 10 pc sample. The total EHZ width for the estimated 10 pc sample is 71.5 AU, including 13.2 AU for the 3 A, 4.9 AU for the 4 F stars, 11.9 AU for the 14 G stars, and 15.4 AU for the 34 K stars. The estimated 384 M stars *en masse* provide

26.1 AU of linear EHZ. This accounts for 36.5% of the total EHZ. Thus, by spectral type, M stars *en masse* provide the largest EHZ real estate.

## 5.2. Predicting the Size of the Habitable Zone from $V - K$ Colors

Given the rapid pace of exoplanet discovery, it would be helpful to have a tool to easily and accurately predict the location of the EHZ to determine whether or not a planet resides within it. Predicting the EHZ of a star based on spectral classification can be problematic due to the inhomogeneity in classification and spectral types being determined over different wavelength ranges. As shown in Henry et al. (2006), the  $V - K$  color is a useful temperature diagnostic for the A through M stars that dominate the solar neighborhood. This relation can also be very helpful in determining a rough estimate of the EHZ based on observable photometry, and may be easily scaled to larger populations.

We use the results from the 5 pc and extended 10 pc samples to derive a relation between  $V - K$  color and the size and location of the EHZ. As in the computation of total habitable real estate, we removed binary stars with unresolved photometry, as well as stars known to be evolved. We do, however, use stars such as Sirius (GJ 244) and Procyon (GJ 280) for which EHZs have been determined, even though their companions corrupt their EHZs. Their white dwarf companions do not significantly contribute to their luminosities or  $V - K$ , and their inclusion improves the statistics of our fit. We fit a second order polynomial, described by Equation 6, to the  $V - K$  colors and computed EHZ widths shown in Figure 4.

$$\text{Log}(EHZ_{\text{width(AU)}}) = 0.648 - 0.457(V - K) + 0.021(V - K)^2 \quad (6)$$

Using the same method, a relationship for  $V - K$  color and the inner and outer radii of the EHZs are described by Equations 7 and 8, respectively. These relations are only valid for main sequence stars.

$$\text{Log}(EHZ_{\text{inner(AU)}}) = 0.593 - 0.457(V - K) + 0.021(V - K)^2 \quad (7)$$

$$\text{Log}(EHZ_{\text{outer(AU)}}) = 0.922 - 0.457(V - K) + 0.021(V - K)^2 \quad (8)$$

As a check on these relations, we use these to calculate the total EHZ width by spectral type of the estimated 10 pc sample and compare these values to the direct calculations described in Sections 4.2 & 4.3. We find the total EHZ widths from the empirical relations

differ on average from the calculated total widths by  $-12.7\%$ ,  $-6.4\%$ ,  $1.6\%$ ,  $4.7\%$ , and  $0.3\%$  for A, F, G, K, and M stars respectively; negative values correspond to underpredictions of the EHZ width totals. The higher percentage differences for A type and F type totals are due to the relatively small populations within 10 pc and the effects of large 2MASS photometric errors due to brightness. The results imply that this relation is useful for quickly estimating the amount of habitable real estate for a population with known  $V - K$  values. We also test how well the predicted inner and outer boundaries from our relations agree for any given star. On average, these predictions yield values consistent to 3% with a dispersion of 22% for both inner and outer boundaries for AFGKM stars in our samples. These dispersions can be interpreted as the uncertainty in the locations of these boundaries from these relations.

### 5.3. Planets in the EHZs of Nearby Stars

Of the 14 confirmed planetary systems within 10 pc of the Sun for which orbits have been determined, five contain multiple planets (GJ 139, GJ 506, GJ 581, GJ 667C, and GJ 876). All 14 systems are listed in Table 11 with published values for semimajor axis and eccentricity, as well as calculated inner and outer radii of the EHZ from this work. Three of the systems, GJ 581, GJ 667C, and GJ 876 have planets in the EHZ.

GJ 581, an M2.5V star at a distance of 6.25 pc, has six proposed planets, but the existence of GJ 581g and GJ 581f are currently debated (see: Vogt et al. 2010; Andrae et al. 2010; Gregory 2011; Anglada-Escudé 2010; Tuomi 2011). If real, GJ 581g, with a semimajor axis of 0.146 AU, orbits in the EHZ in a presumed circular orbit. Using the CHARA Array, von Braun et al. (2011) recently measured the size of the star and derived HZ boundaries of  $R_{in} = 0.11$  AU and  $R_{out} = 0.21$  AU. Our EHZ is somewhat closer in to the star,  $R_{in} = 0.083$  AU and  $R_{out} = 0.179$  AU, but still places GJ 581g in the EHZ. The differences are due to our calculated luminosity ( $L = 0.11L_{\odot}$ ) being 8% lower than von Braun et al. (2011), as they adopted an extinction of  $A_V = 0.174$  for GJ 581, which they note as unexpected for a star at this distance. GJ 581d, with semimajor axis of 0.22 AU and eccentricity of 0.38, also moves in and out of the EHZ of GJ 581.

GJ 667C, an M1.5V star at a distance of 7.23 pc, hosts two planets, and possibly four (Anglada-Escudé et al. 2012). Although GJ 667Cb does not lie within the EHZ, GJ 667Cc ( $m \sin i$  of  $4.5 M_{\oplus}$ ) lies within the EHZ for the majority of its orbit. With a semimajor axis of 0.123 AU and eccentricity  $< 0.27$ , it may lie completely within the EHZ once the eccentricity is more highly constrained.

GJ 876, an M3.5V star at a distance of 4.66 pc, hosts four planets (Rivera et al. 2010).

Our calculations show an EHZ spanning 0.090-0.191 AU. Rivera et al. (2010) report orbital fits for two planets near the EHZ with semimajor axes of 0.13 AU (GJ 876c) and 0.21 AU (GJ 876b), and eccentricities of 0.25 and 0.03, respectively. As shown in Figure 5, this allows for GJ 876c to be in the EHZ of its host star for the full duration of its orbit, while GJ 876b lies just outside the EHZ. Although these planets are not considered terrestrial ( $m \sin i$  of 0.56 and 1.89  $M_J$ ), the possibility exists that they could have terrestrial-like moons that could be habitable.

#### 5.4. Complications to Habitability

The previous sections provide estimates of EHZs based on the requirement of liquid water on a planetary surface. Of course, a planet’s location in the EHZ of a host star does not guarantee its habitability. A host of other factors, such as planet size, atmosphere, magnetic fields, and even plate tectonics, play vital roles in determining the habitability of a planet in the EHZ. Without a sufficiently thick atmosphere, biologically harmful radiation can penetrate to the surface of a planet. On Earth, atmospheric  $CO_2$  levels are kept in check by the carbon-silicate cycle. Known to regulate climate temperatures through a negative feedback, this cycle allows for as much as 60 bars (Kasting 1996) of  $CO_2$  to be locked away in rock and sediments. This slow carbon-silicate cycle requires that water be present, because without water, the atmospheric  $CO_2$  cannot be sequestered as carbonate. A magnetosphere on Earth also plays an important role by deflecting harmful charged particles. Tectonic activity may be one of the key factors in keeping a planet habitable (Doyle et al. 1998). Without water, the lithosphere of a planet may become a stagnant lid, halting tectonic activity and the sequestration of  $CO_2$ .

There is a temporal constraint on habitability as well, as the HZ may change considerably over the lifetime of a star (Kasting et al. 1993; Kasting 1996; Tarter et al. 2007; Selsis et al. 2007). Putting these complications aside, the requirement of liquid water on the surface of a planet is a good first order approximation to habitability.

## 6. Summary

We assess the sample of stars currently known to be within 5 pc of the Sun for the purpose of determining the habitable real estate and its dependence on spectral type. Because of the sparse population of high mass stars within 5 pc of the Sun, we expand this sample for AFGK stars to 10 pc; there are no O or B stars within 10 pc of the Sun. After



eliminating evolved stars, substellar objects, and close multiples in which planets in HZs would be dynamically unstable, we use the final sample to estimate the EHZs for stars in both the 5 pc and extended 10 pc samples. We do not consider circumbinary habitable zones in this work, but EHZs are calculated in the same fashion as single stars for each of the 49 components in multiple systems that satisfy our dynamical stability constraint.

Using PHOENIX models convolved with filter response curves, we fit observed  $UBVRIJHK$  photometry for each object, assuming spherical, non-rapidly rotating stars with solar metallicity and  $\log g$  values of 4.0 to 5.0, with the 2 exceptions being the metal poor stars GJ 191 and GJ 451. This fitting process allows us to determine a radius and  $T_{eff}$  for each star that is then used to determine its surrounding EHZ, calculated using a modified “Venus and early Mars criterion” from Selsis et al. (2007).

We use estimates of linear AU to map the EHZ of each star and sum by spectral type *en masse*: 48 M dwarf stars used in the 5 pc sample provide more habitable real estate (3.3 AU) than the three G dwarf stars (2.6 AU) and seven K stars (2.9 AU) found within 5 pc of the Sun. Even after extending the sample of AFGK stars to 10 pc, the anticipated sample of M dwarfs within 10 pc (not all have yet been identified) possess more EHZ real estate than any other spectral type, spanning  $\sim 26$  AU compared to 13.2 AU, 11.9 AU, and 15.4 AU for each of the A, G, and K types (the F stars provide only 4.9 linear AU of EHZ). The result is a natural consequence of the large relative numbers of M dwarfs, and the frequency of close companions that declines with mass.

As a population M dwarfs provide more options and more habitable real estate than their more massive counterparts. Furthermore, recent results from Kepler show that for stars with  $T_{eff} < 4000\text{K}$  within 5 pc of the Sun, there is likely to be at least 2 Earth-size planets in the HZ. That number increases to 16 within 10 pc (Dressing & Charbonneau 2013).

Using the 5 pc and extended 10 pc samples, we derive relations between  $V - K$  color and EHZ width and inner and outer limits. Comparisons of color predicted locations suggest they are comparable to uncertainties associated with habitability assumptions (e.g., Section 4.2). Thus, these color relations are practical tools for estimating the EHZs of stars using commonly available photometric measurements. The relations for the inner and outer radii of the EHZ are helpful for quickly estimating whether or not a known planet or disk is within the EHZ. The relation for EHZ size is useful in predicting the habitable real estate available in a stellar population. In particular, we consider the results for the 14 extrasolar planetary systems known within 10 pc of the Sun. The three systems with planets in the calculated EHZs — GJ 581, GJ 667C, and GJ 876 — are all M dwarfs. In total, as many as four planets circling these stars spend at least part of their time in the EHZs, providing an ideal set of targets for future efforts to detect biosignatures.

### 6.1. Acknowledgments

The authors would like to thank J. Kasting for extremely helpful advice and guidance. We would also like to thank the RECONS team for the generous amount of data and support provided. Data used in this paper were acquired via support from the National Science Foundation (grants AST 05-07711 and AST 09-08402) and through the continuous cooperation of the SMARTS Consortium. This project was funded in part by NSF/AAG grant no. 0908018. This research has made use of the SIMBAD database, operated at CDS, Strasbourg, France, data from the Two Micron All Sky Survey, which is a joint project of the University of Massachusetts and IPAC, funded by NASA and NSF, and the Sixth Catalog of Orbits of Visual Binary Stars, operated by the US Naval Observatory.

## REFERENCES

- Absil, O., di Folco, E., Mérand, A., et al. 2008, *A&A*, 487, 1041
- Alonso, A., Arribas, S., & Martinez-Roger, C. 1995, *A&A*, 297, 197
- Andrae, R., Schulze-Hartung, T., & Melchior, P. 2010, arXiv:1012.3754
- Anglada-Escudé, G., Arriagada, P., Vogt, S. S., et al. 2012, *ApJ*, 751, L16
- Anglada-Escudé, G. 2010, arXiv:1011.0186
- Aufdenberg, J. P., et al. 2006, *ApJ*, 651, 617
- Bailey, J., Butler, R. P., Tinney, C. G., Jones, H. R. A., O’Toole, S., Carter, B. D., & Marcy, G. W. 2009, *ApJ*, 690, 743
- Baize, P., & Petit, M. 1989, *A&AS*, 77, 497
- Baize, P. 1950, *Journal des Observateurs*, 33, 1
- Baraffe, I., Chabrier, G., Allard, F., & Hauschildt, P. H. 1998, *A&A*, 337, 403
- Barbieri, M., Marzari, F., & Scholl, H. 2002, *A&A*, 396, 219
- Barnes, R., Jackson, B., Greenberg, R., & Raymond, S. N. 2009, *ApJ*, 700, L30
- Batten, A. H., Fletcher, J. M., & MacCarthy, D. G. 1989, *Publications of the Dominion Astrophysical Observatory Victoria*, 17, 1
- Benedict, G. F., et al. 1999, *AJ*, 118, 1086
- Benedict, G. F., et al. 2002, *ApJ*, 581, L115
- Benedict, G. F., et al. 2006, *AJ*, 132, 2206
- Berger, D. H., et al. 2006, *ApJ*, 644, 475
- Bessell, M. S., Castelli, F., & Plez, B. 1998, *A&A*, 333, 231
- Bessel, M. S. 1990, *A&AS*, 83, 357
- Bessel, M. S. 1991, *AJ*, 101, 662
- Biller, B. A., Kasper, M., Close, L. M., Brandner, W., & Kellner, S. 2006, *ApJ*, 641, L141
- Bonfils, X., et al. 2007, *A&A*, 474, 293

- Borucki, W. J., & for the Kepler Team 2010, arXiv:1006.2799
- Boyajian, T. S., von Braun, K., van Belle, G., et al. 2012, arXiv:1208.2431
- Breckinridge, J. B., & Kron, G. E. 1964, *PASP*, 76, 139
- Burgasser, A. J., et al. 2000, *ApJ*, 531, L57
- Butler, R. P., et al. 2006, *ApJ*, 646, 505
- Butler, R. P., Johnson, J. A., Marcy, G. W., Wright, J. T., Vogt, S. S., & Fischer, D. A. 2006, *PASP*, 118, 1685
- Carpenter, J. M. 2001, *AJ*, 121, 2851
- Chance, D. R., & Hershey, J. L. 1998, *PASP*, 110, 425
- Cohen, M., Wheaton, W. A., & Megeath, S. T. 2003, *AJ*, 126, 1090
- Costa, E., Méndez, R. A., Jao, W.-C., Henry, T. J., Subasavage, J. P., Brown, M. A., Ianna, P. A., & Bartlett, J. 2005, *AJ*, 130, 337
- Costa, E., Méndez, R. A., Jao, W.-C., Henry, T. J., Subasavage, J. P., & Ianna, P. A. 2006, *AJ*, 132, 1234
- Couteau, P. 1959, *Bulletin Astronomique*, 23, 127
- Cutri, R. M., et al. 2003, The IRSA 2MASS All-Sky Point Source Catalog, NASA/IPAC Infrared Science Archive.<http://irsa.ipac.caltech.edu/applications/Gator/>
- Deacon, N. R., & Hambly, N. C. 2007, *A&A*, 468, 163
- Deacon, N. R., Hambly, N. C., Henry, T. J., Subasavage, J. P., Brown, M. A., & Jao, W.-C. 2005, *AJ*, 129, 409
- Delfosse, X., Forveille, T., Udry, S., Beuzit, J.-L., Mayor, M., & Perrier, C. 1999, *A&A*, 350, L39
- Demory, B.-O., et al. 2009, *A&A*, 505, 205
- Di Folco, E., Thévenin, F., Kervella, P., Domiciano de Souza, A., Coudé du Foresto, V., Ségransan, D., & Morel, P. 2004, *A&A*, 426, 601
- Doyle, L. R., Billingham, J., Devinenzi, D. L., 1998, *Acta Astronautica*, 42, 399

- Dressing, C. D., & Charbonneau, D. 2013, *ApJ*, 767, 95
- Drummond, J. D., Christou, J. C., & Fugate, R. Q. 1995, *ApJ*, 450, 380
- Dumusque, X., Pepe, F., Lovis, C., et al. 2012, *Nature*, 491, 207
- Eggen, O. J. 1956, *AJ*, 61, 405
- Eggen, O. J. 1965, *AJ*, 70, 19
- Eggen, O. J. 1996, *AJ*, 111, 466
- Eggenberger, A., Udry, S., Chauvin, G., Beuzit, J.-L., Lagrange, A.-M., Ségransan, D., & Mayor, M. 2007, *A&A*, 474, 273
- Farrington, C. D., et al. 2010, *AJ*, 139, 2308
- Fekel, F. C. 1997, *PASP*, 109, 514
- Forveille, T., et al. 1999, *A&A*, 351, 619
- Forveille, T., et al. 2009, *A&A*, 493, 645
- Fuhrmann, K., Pfeiffer, M., Frank, C., Reetz, J., & Gehren, T. 1997, *A&A*, 323, 909
- Gatewood, G. D., & Gatewood, C. V. 1978, *ApJ*, 225, 191
- Gatewood, G., Stein, J., de Jonge, J. K., Persinger, T., Reiland, T., & Stephenson, B. 1992, *AJ*, 104, 1237
- Gatewood, G., de Jonge, K. J., & Stephenson, B. 1993, *PASP*, 105, 1101
- Gatewood, G., Coban, L., & Han, I. 2003, *AJ*, 125, 1530
- Gatewood, G. 1989, *AJ*, 97, 1189
- Gatewood, G. 1994, *PASP*, 106, 138
- Geyer, D. W., Harrington, R. S., & Worley, C. E. 1988, *AJ*, 95, 1841
- Glass, I. S. 1975, *MNRAS*, 171, 19P
- Gliese, W., & Jahreiß, H. 1991, On: The Astronomical Data Center CD-ROM: Selected Astronomical Catalogs, Vol. I; L.E. Brozmann, S.E. Gesser (eds.), NASA/Astronomical Data Center, Goddard Space Flight Center, Greenbelt, MD,

- Golimowski, D. A., Henry, T. J., Krist, J. E., Schroeder, D. J., Marcy, G. W., Fischer, D. A., & Butler, R. P. 2000, *AJ*, 120, 2082
- Gould, A. 2003, *AJ*, 126, 472
- Gray, R. O., Napier, M. G., & Winkler, L. I. 2001, *AJ*, 121, 2148
- Gray, R. O., Corbally, C. J., Garrison, R. F., McFadden, M. T., Bubar, E. J., McGahee, C. E., O’Donoghue, A. A., & Knox, E. R. 2006, *AJ*, 132, 161
- Gregory, P. C. 2011, arXiv:1101.0800
- Greissl, J., Meyer, M. R., Wilking, B. A., Fanetti, T., Schneider, G., Greene, T. P., & Young, E. 2007, *AJ*, 133, 1321
- Hale, A. 1994, *AJ*, 107, 306
- Han, I., & Gatewood, G. 2002, *PASP*, 114, 224
- Hauschildt, P. H., Allard, F., & Baron, E. 1999, *ApJ*, 512, 377
- Heintz, W. D. 1974, *AJ*, 79, 819
- Heintz, W. D. 1986, *AJ*, 92, 446
- Heintz, W. D. 1987, *PASP*, 99, 1084
- Heintz, W. D. 1994, *AJ*, 108, 2338
- Heintz, W. D. 1996, *AJ*, 111, 412
- Henry, T.J. 2010, in *Royal Astronomical Society of Canada Observer’s Handbook 2010*, ed. Patrick Kelly. Toronto: Royal Astronomical Society of Canada
- Henry, T.J. 2012, in *Royal Astronomical Society of Canada Observer’s Handbook 2012*, ed. David M.F. Chapman. Toronto: Royal Astronomical Society of Canada
- Henry, T. J., & McCarthy, D. W., Jr. 1993, *AJ*, 106, 773
- Henry, T. J., Kirkpatrick, J. D., & Simons, D. A. 1994, *AJ*, 108, 1437
- Henry, T. J., Ianna, P. A., Kirkpatrick, J. D., & Jahreiss, H. 1997, *AJ*, 114, 388
- Henry, T. J., Walkowicz, L. M., Barto, T. C., & Golimowski, D. A. 2002, *AJ*, 123, 2002

- Henry, T. J., Subasavage, J. P., Brown, M. A., Beaulieu, T. D., Jao, W.-C., & Hambly, N. C. 2004, *AJ*, 128, 2460
- Henry, T. J., Jao, W.-C., Subasavage, J. P., Beaulieu, T. D., Ianna, P. A., Costa, E., & Méndez, R. A. 2006, *AJ*, 132, 2360
- Howard, A. W., et al. 2010, arXiv:1011.0414
- Howard, A. W., Marcy, G. W., Bryson, S. T., et al. 2012, *ApJS*, 201, 15
- Huang, S.-S. 1959, *PASP*, 71, 421
- Høg, E., et al. 2000, *A&A*, 355, L27
- Irwin, A. W., Fletcher, J. M., Yang, S. L. S., Walker, G. A. H., & Goodenough, C. 1992, *PASP*, 104, 489
- Irwin, A. W., Yang, S. L. S., & Walker, G. A. H. 1996, *PASP*, 108, 580
- Jao, W.-C., Henry, T. J., Subasavage, J. P., Brown, M. A., Ianna, P. A., Bartlett, J. L., Costa, E., & Méndez, R. A. 2005, *AJ*, 129, 1954
- Jao, W.-C., Henry, T. J., Beaulieu, T. D., & Subasavage, J. P. 2008, *AJ*, 136, 840
- Johnson, H. L., & Morgan, W. W. 1953, *ApJ*, 117, 313
- Johnson, H. L., & Morgan, W. W. 1953, *ApJ*, 117, 313
- Johnson, H. L., Iriarte, B., Mitchell, R. I., & Wisniewski, W. Z. 1966, *Communications of the Lunar and Planetary Laboratory*, 4, 99
- Johnson, H. L., MacArthur, J. W., & Mitchell, R. I. 1968, *ApJ*, 152, 465
- Johnson, J. A., Butler, R. P., Marcy, G. W., et al. 2007, *ApJ*, 670, 833
- Johnson, J. A., et al. 2010, *PASP*, 122, 149
- Kalas, P., Graham, J. R., Chiang, E., et al. 2008, *Science*, 322, 1345
- Kaltenegger, L., Fridlund, M., & Kasting, J. 2002, *ESA SP-514: Earth-like Planets and Moons*, 277
- Kaltenegger, L. 2010, *ApJ*, 712, L125
- Kasting, J. F. 1996, *Ap&SS*, 241, 3

- Kasting, J. F., Whitmire, D. P., & Reynolds, R. T. 1993, *Icarus*, 101, 108
- Kenyon, S. J., & Hartmann, L. 1995, *ApJS*, 101, 117
- Kervella, P., & Fouqué, P. 2008, *A&A*, 491, 855
- Kervella, P., Thévenin, F., Morel, P., Bordé, P., & Di Folco, E. 2003, *A&A*, 408, 681
- Kervella, P., Thévenin, F., Morel, P., Berthomieu, G., Provost, J., Bordé, P., & Ségransan, D. 2003, *Solar and Solar-Like Oscillations: Insights and Challenges for the Sun and Stars*, 25th meeting of the IAU, Joint Discussion 12, 18 July 2003, Sydney, Australia, 12
- Kervella, P., et al. 2008, *A&A*, 488, 667
- Kidder, K. M., Holberg, J. B., & Mason, P. A. 1991, *AJ*, 101, 579
- Kirkpatrick, J. D., Dahn, C. C., Monet, D. G., Reid, I. N., Gizis, J. E., Liebert, J., & Burgasser, A. J. 2001, *AJ*, 121, 3235
- Koch, D. G., et al. 2004, *Proc. SPIE*, 5487, 1491
- Landolt, A. U. 1992, *AJ*, 104, 372
- Lane, B. F., Boden, A. F., & Kulkarni, S. R. 2001, *ApJ*, 551, L81
- Lee, J. W., Kim, S.-L., Kim, C.-H., Koch, R. H., Lee, C.-U., Kim, H.-I., & Park, J.-H. 2009, *AJ*, 137, 3181
- Leggett, S. K. 1992, *ApJS*, 82, 351
- Leinert, C., Haas, M., Allard, F., et al. 1990, *A&A*, 236, 399
- Lowell, P. 1895, *Popular Astronomy*, 2, 255
- Lutz, T. E. 1971, *PASP*, 83, 488
- Luyten, W. J. 1957, *Minneapolis, Lund Press, 1957.*,
- Lépine, S., & Shara, M. M. 2005, *AJ*, 129, 1483
- Malin, M. C., & Edgett, K. S. 2000, *Science*, 288, 2330
- Marcy, G. W., Butler, R. P., Fischer, D., Vogt, S. S., Lissauer, J. J., & Rivera, E. J. 2001, *ApJ*, 556, 296



- Marion, G. M., Fritsen, C. H., Eicken, H., & Payne, M. C. 2003, *Astrobiology*, 3, 785
- Mason, B. D., & Hartkopf, W. I. 2006, *Journal of Double Star Observations*, 2, 171
- Mason, B. D., McAlister, H. A., Hartkopf, W. I., & Shara, M. M. 1995, *AJ*, 109, 332
- Mayor, M., et al. 2009, *A&A*, 507, 487
- McCaughrean, M. J., Close, L. M., Scholz, R.-D., Lenzen, R., Biller, B., Brandner, W., Hartung, M., & Lodieu, N. 2004, *A&A*, 413, 1029
- Mermilliod, J.-C. 1986, *Catalogue of Eggen's UBV data.*, 0 (1986), 0
- Monet, D. G., et al. 2003, *AJ*, 125, 984
- Monnier, J. D., Zhao, M., Pedretti, E., et al. 2007, *Science*, 317, 342
- Montes, D., Ramirez, L. W., & Welty, A. D. 1999, *ApJS*, 123, 283
- Montes, D., López-Santiago, J., Gálvez, M. C., Fernández-Figueroa, M. J., De Castro, E., & Cornide, M. 2001, *MNRAS*, 328, 45
- Mould, J. R., & Hyland, A. R. 1976, *ApJ*, 208, 399
- Oja, T. 1984, *A&AS*, 57, 357
- Oja, T. 1993, *A&AS*, 100, 591
- Parkinson, C. D., Liang, M.-C., Hartman, H., Hansen, C. J., Tinetti, G., Meadows, V., Kirschvink, J. L., & Yung, Y. L. 2007, *A&A*, 463, 353
- Pasquini, L., Liu, Q., & Pallavicini, R. 1994, *A&A*, 287, 191
- Patience, J., et al. 2002, *ApJ*, 581, 654
- Pepe, F., Lovis, C., Ségransan, D., et al. 2011, *A&A*, 534, A58
- Perryman, M. A. C., Lindgren, L., Kovalevsky, J., et al. 1997, *A&A*, 323, L49
- Pourbaix, D., et al. 2002, *A&A*, 386, 280
- Pourbaix, D. 2000, *A&AS*, 145, 215
- Poveda, A., Herrera, M. A., Allen, C., Cordero, G., & Lavalley, C. 1994, *Rev. Mexicana Astron. Astrofis.*, 28, 43

- Qian, S.-B., Liao, W.-P., Zhu, L.-Y., & Dai, Z.-B. 2010, *ApJ*, 708, L66
- Quintana, E. V., Adams, F. C., Lissauer, J. J., & Chambers, J. E. 2007, *ApJ*, 660, 807
- Raghavan, D., Henry, T. J., Mason, B. D., Subasavage, J. P., Jao, W.-C., Beaulieu, T. D., & Hambly, N. C. 2006, *ApJ*, 646, 523
- Raghavan, D., et al. 2010, *ApJS*, 190, 1
- Reid, I. N., & Gizis, J. E. 1997, *AJ*, 113, 2246
- Reid, I. N., Hawley, S. L., & Gizis, J. E. 1995, *AJ*, 110, 1838
- Reid, I. N., et al. 2004, *AJ*, 128, 463
- Rivera, E. J., Laughlin, G., Butler, R. P., Vogt, S. S., Haghighipour, N., & Meschiari, S. 2010, *ApJ*, 719, 890
- Royer, F., Gerbaldi, M., Faraggiana, R., & Gómez, A. E. 2002, *A&A*, 381, 105
- Royer, F., Zorec, J., & Gómez, A. E. 2007, *A&A*, 463, 671
- Ruck, M. J., & Smith, G. 1995, *A&A*, 304, 449
- Schmidt, S. J., Cruz, K. L., Bongiorno, B. J., Liebert, J., & Reid, I. N. 2007, *AJ*, 133, 2258
- Scholz, R.-D., McCaughrean, M. J., Lodieu, N., & Kuhlbrodt, B. 2003, *A&A*, 398, L29
- Selsis, F., Kasting, J. F., Levrard, B., Paillet, J., Ribas, I., & Delfosse, X. 2007, *A&A*, 476, 1373
- Strand, K. A. 1969, *AJ*, 74, 760
- Subasavage, J. P., Jao, W.-C., Henry, T. J., Bergeron, P., Dufour, P., Ianna, P. A., Costa, E., & Méndez, R. A. 2009, *AJ*, 137, 4547
- Söderhjelm, S. 1999, *A&A*, 341, 121
- Söderhjelm, S. 1999, *A&A*, 341, 121
- Ségransan, D., Delfosse, X., Forveille, T., Beuzit, J.-L., Udry, S., Perrier, C., & Mayor, M. 2000, *A&A*, 364, 665
- Ségransan, D., Kervella, P., Forveille, T., & Queloz, D. 2003, *A&A*, 397, L5
- Tarter, J. C., et al. 2007, *Astrobiology*, 7, 30

- Tinney, C. G., Butler, R. P., Jones, H. R. A., Wittenmyer, R. A., O’Toole, S., Bailey, J., & Carter, B. D. 2011, *ApJ*, 727, 103
- Tokovinin, A. A. 1997, *A&AS*, 124, 75
- Torres, G., Henry, T. J., Franz, O. G., & Wasserman, L. H. 1999, *AJ*, 117, 562
- Torres, C. A. O., Quast, G. R., da Silva, L., de La Reza, R., Melo, C. H. F., & Sterzik, M. 2006, *A&A*, 460, 695
- Tuomi, M. 2011, *A&A*, 528, L5
- Turner, N. H., ten Brummelaar, T. A., McAlister, H. A., Mason, B. D., Hartkopf, W. I., & Roberts, L. C., Jr. 2001, *AJ*, 121, 3254
- Vogt, S. S., et al. 2010, *ApJ*, 708, 1366
- Vogt, S. S., Butler, R. P., Rivera, E. J., Haghighipour, N., Henry, G. W., & Williamson, M. H. 2010, *ApJ*, 723, 954
- Weidner, C., & Horne, K. 2010, *A&A*, 521, A76
- Weis, E. W. 1993, *AJ*, 105, 1962
- Weis, E. W. 1996, *AJ*, 112, 2300
- Wiegert, P. A., & Holman, M. J. 1997, *AJ*, 113, 1445
- Wieth-Knudsen, N. *Inf. Circ.* 13, 1957
- Wilson, O. C. 1966, *ApJ*, 144, 695
- Woolf, V. M., & Wallerstein, G. 2005, *MNRAS*, 356, 963
- Worley, C. E., & Behall, A. L. 1973, *AJ*, 78, 650
- van Albada, G. B. 1957, *Contributions from the Bosscha Observatory*, 5, 1
- van Altena, W. F., Lee, J. T., & Hoffleit, E. D. 1995, *The General Catalogue of Trigonometric Stellar Parallaxes*, New Haven, CT: Yale University Observatory, 1995, 4th ed.
- Valenti, J. A., & Fischer, D. A. 2005, *VizieR Online Data Catalog*, 215, 90141
- von Braun, K., Boyajian, T. S., Kane, S. R., et al. 2011, *ApJ*, 729, L26

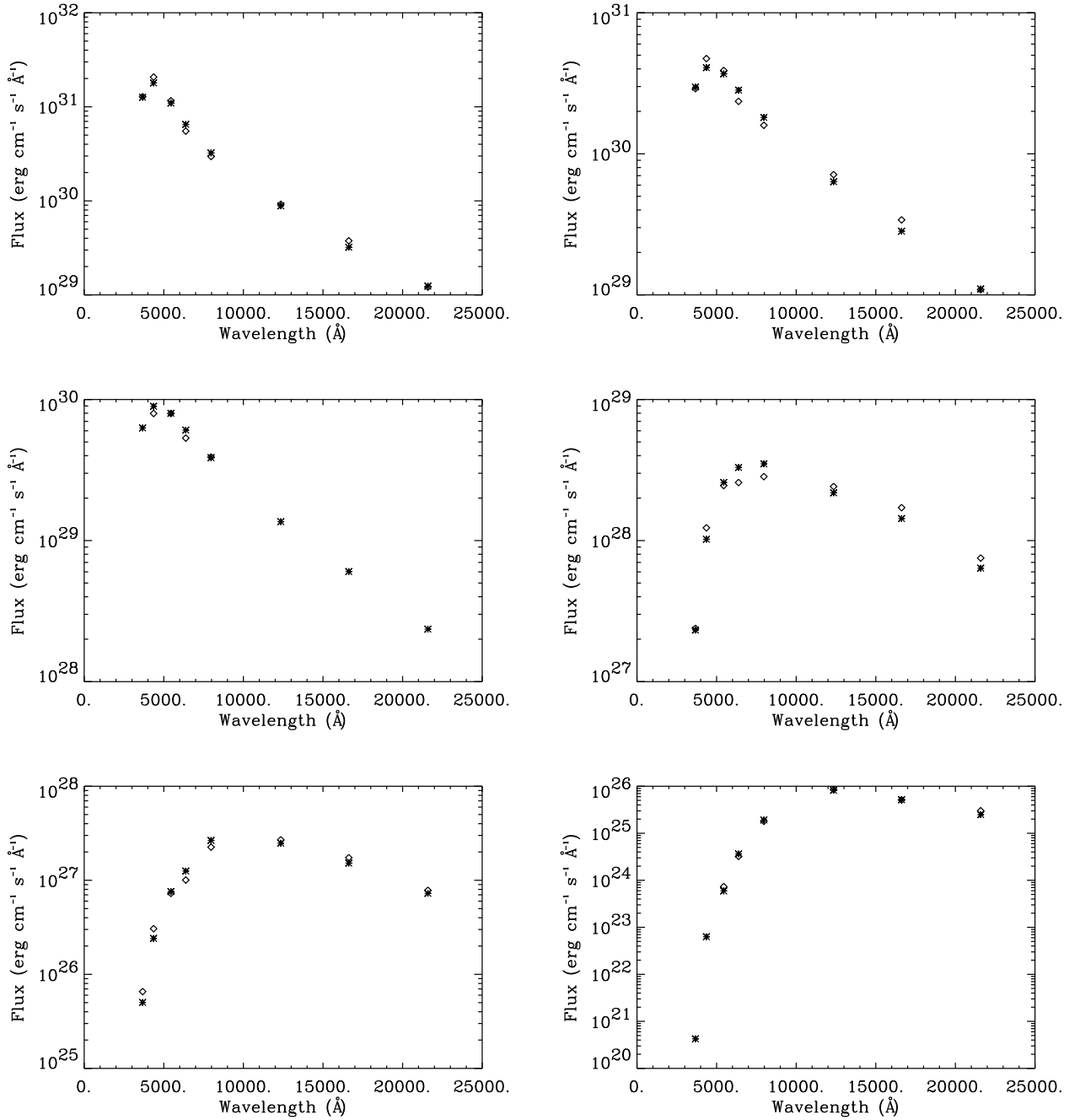


Fig. 1.— Examples of model (\*) and observed (◇) flux values are shown for (*top-left to right*) GJ 244A (A1.0V), GJ 280A (F5.0IV–V), (*middle-left to right*) GJ 599A (G2.0V), GJ 380 (K7.0V), (*bottom-left to right*) GJ 273 (M3.5V), SCR 1845-6357A (M8.5V). In each case the points represent *UBVRIJK* photometry. Model values for stars with incomplete photometry, e.g., GJ 559A missing *UJHK* and SCR 1845-6357A missing *UB*, are plotted for completeness.

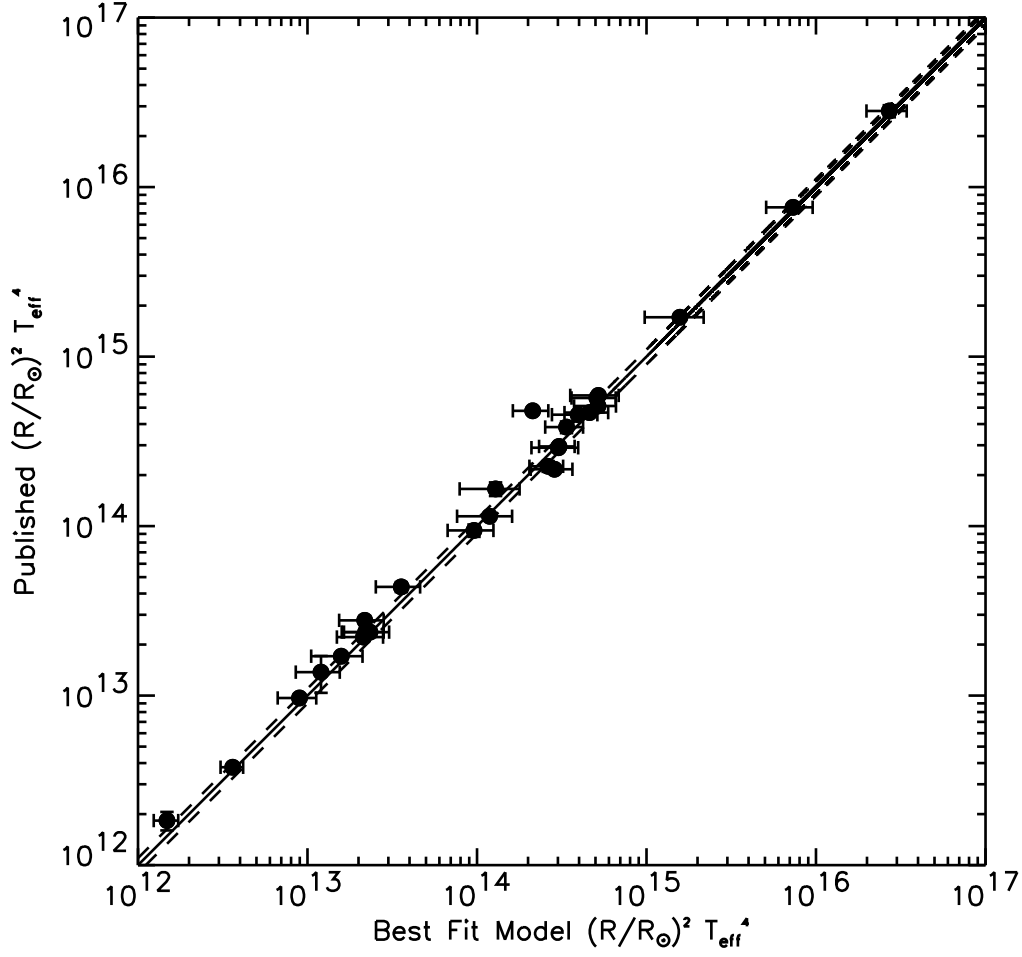


Fig. 2.— Model fits vs published  $(R/R_{\odot})^2 T^4$  values. The solid line illustrates 1:1 agreement and the dashed lines represent 10% offsets. Error bars are  $1\sigma$  for the model and given errors for the interferometrically derived values used to derive the published values.

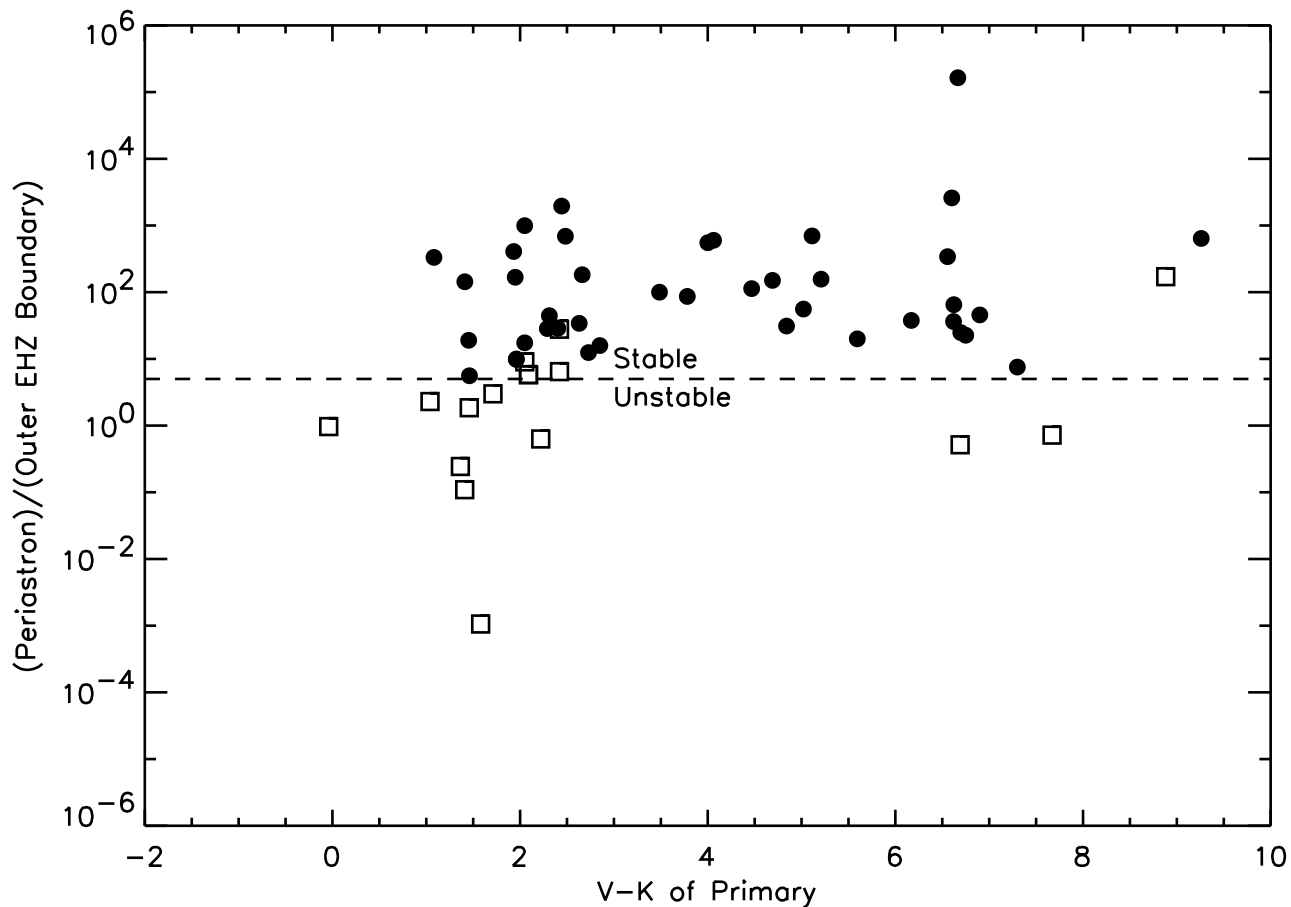


Fig. 3.— The closest approach of a companion star to the outer radius of the EHZ is plotted versus the primary’s  $V-K$  value. Photometrically unresolved multiples are plotted as *open squares*, while resolved components are plotted as *filled circles*. Stars with companions that get closer than 5 times the outer EHZ boundary (*dashed line*) are considered dynamically unstable planet hosts, and are not included in the total habitable real estate calculations. GJ 663AB and GJ 663BA are plotted as the same point as their  $\Delta V$  and  $\Delta K = 0$ . The open square at  $V - K = 8.88$ , ratio = 173, is SCR 1845-6357, an M dwarf with a brown dwarf companion in a highly uncertain orbit.

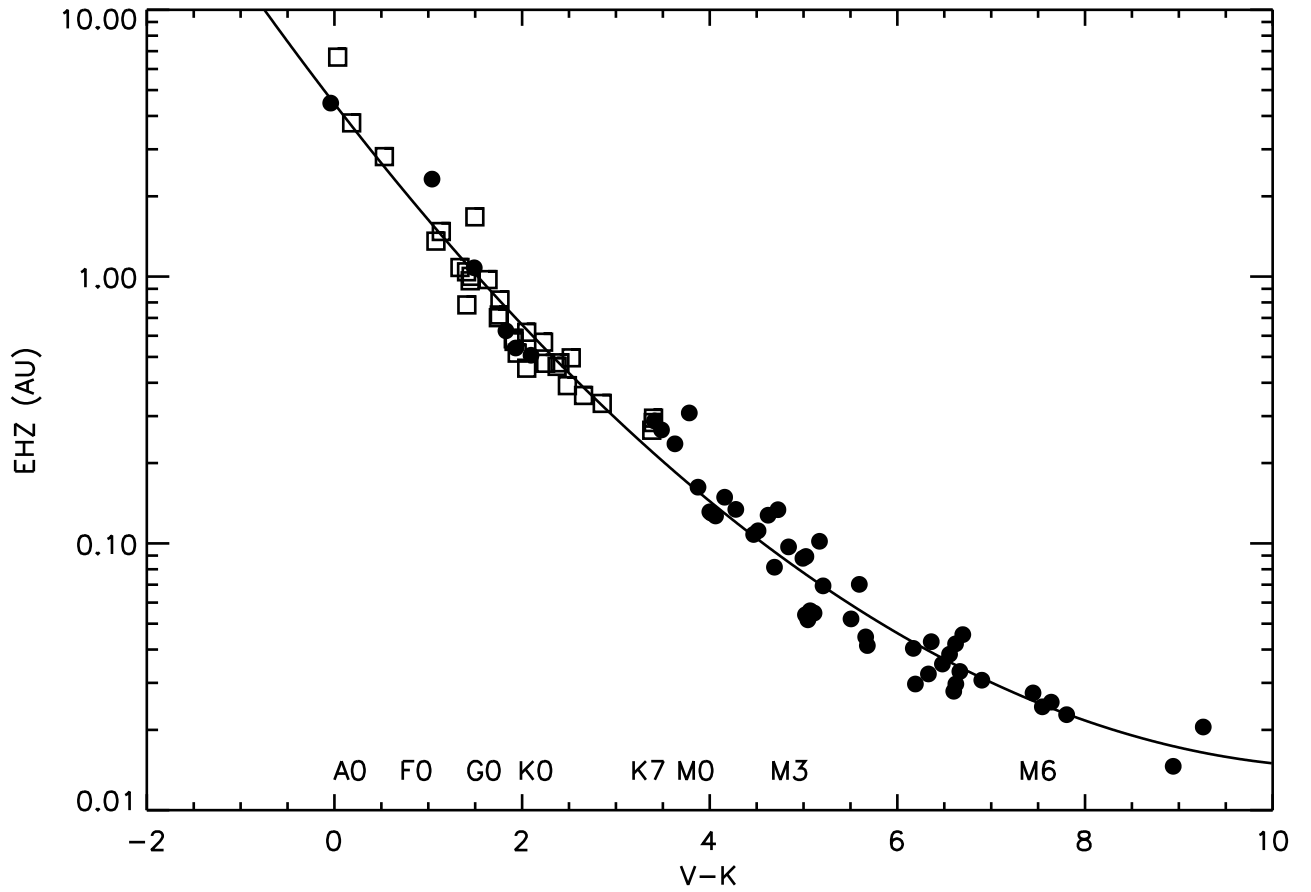


Fig. 4.— Empirical habitable zone (EHZ) widths for the 5 pc (*filled circles*) and extended 10 pc samples (*open squares*). The best fit relation (Equation 6 in text) is overplotted.

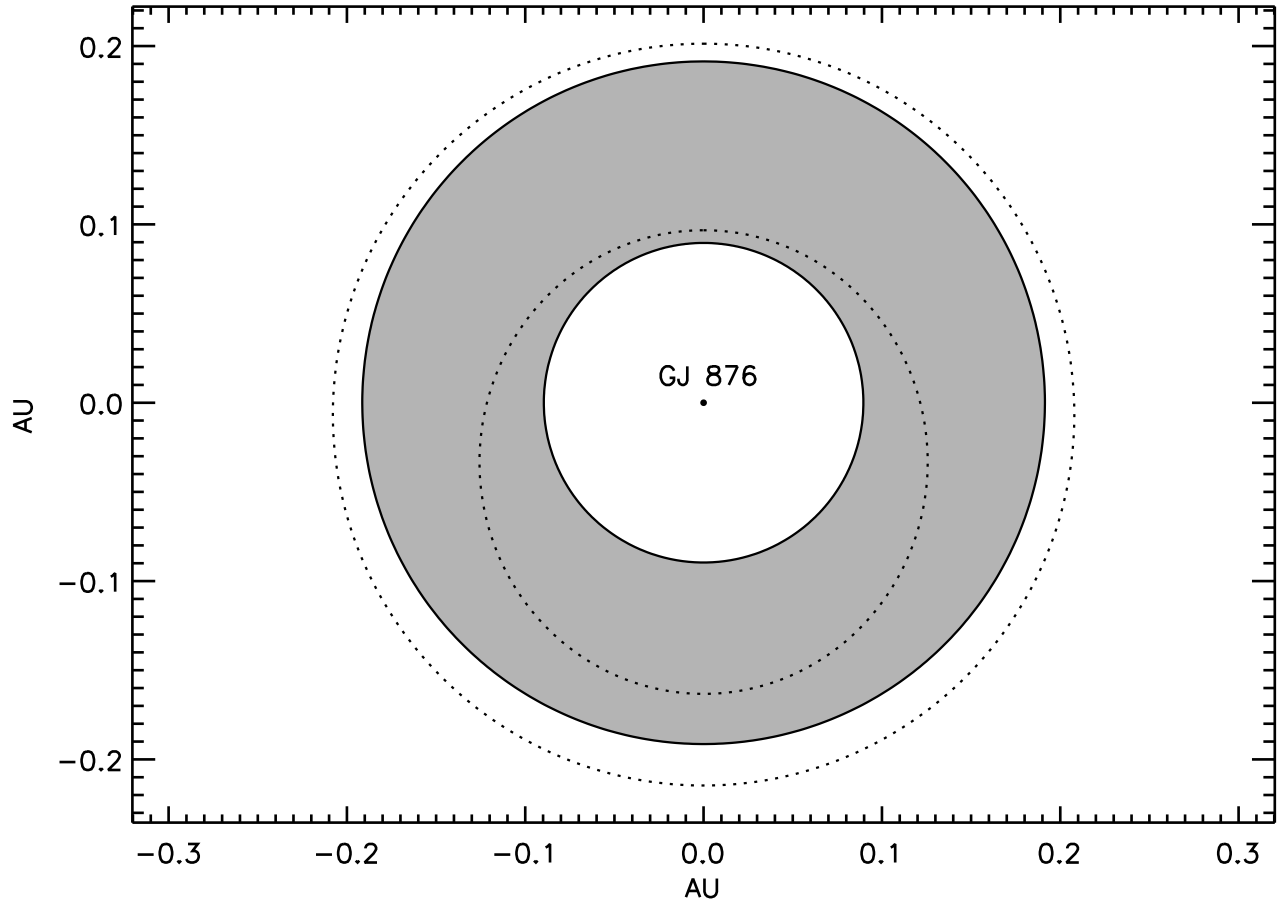


Fig. 5.— The EHZ in this figure is shown as a shaded disk, along with the orbits of the two planets (dotted circles) in the GJ 876 system nearest the EHZ.



Table 1. Five Parsec Sample

Name	LHS	RA 2000.0	DEC	$\pi$	err	# of $\pi$	SpType	Ref
Sun	...	...	...	...	...	...	G2.0V	...
GJ 1	1	00 05 24.4	-37 21 27	.23032	.00090	2	M1.5V	Hen10
GJ 1002	2	00 06 43.2	-07 32 17	.21300	.00360	1	M5.0V	Hen94
GJ 15 A	3	00 18 22.9	+44 01 23	.27987	.00060	3	M1.5V	Hen94
GJ 15 B	4	00 18 22.9	+44 01 23	.27987	.00060	3	M3.5V	Hen94
GJ 35	7	00 49 09.9	+05 23 19	.23270	.00181	2	DZ7	YPC95
GJ 54.1	138	01 12 30.6	-16 59 57	.26908	.00299	2	M4.5V	Hen94
GJ 65 A	9	01 39 01.3	-17 57 01	.37370	.00270	1	M5.5V	Hen94
GJ 65 B	10	01 39 01.3	-17 57 01	.37370	.00270	1	M6.0V	Hen94
GJ 71	146	01 44 04.1	-15 56 15	.27397	.00017	2	G8.5V	Gra06
GJ 83.1	11	02 00 13.2	+13 03 08	.22480	.00290	1	M4.5V	Hen94
SO 0253+1652	...	02 53 00.9	+16 52 53	.25941	.00089	3	M7.0V	Hen04
DEN 0255-4700	...	02 55 03.7	-47 00 52	.20137	.00389	1	L7.5V	Cos06
GJ 144	1557	03 32 55.8	-09 27 30	.31122	.00009	3	K2.0V	Gra06
GJ 1061	1565	03 36 00.0	-44 30 46	.27201	.00130	2	M5.0V	Hen06
LP 944-020	...	03 39 35.2	-35 25 41	.20140	.00421	1	M9.0V	Sch07
GJ 166 A	23	04 15 16.3	-07 39 10	.20065	.00023	2	K0.5V	Gra06
GJ 166 B	24	04 15 22.0	-07 39 35	.20065	.00023	2	DA4	CNS91
GJ 166 C	25	04 15 22.0	-07 39 35	.20065	.00023	2	M4.5V	Hen94
GJ 191	29	05 11 40.6	-45 01 06	.25567	.00091	2	M2.0VI	Jao08
GJ 234 A	1849	06 29 23.4	-02 48 50	.24444	.00092	3	M4.0V	Mon01
GJ 234 B	1850	06 29 23.4	-02 48 50	.24444	.00092	3	M5.5V	Rei04
GJ 244 A	219	06 45 08.9	-16 42 58	.38002	.00128	2	A1.0V	Joh53
GJ 244 B	...	06 45 08.9	-16 42 58	.38002	.00128	2	DA2	CNS91
GJ 273	33	07 27 24.5	+05 13 33	.26623	.00066	3	M3.5V	Hen94
GJ 280 A	233	07 39 18.1	+05 13 30	.28517	.00064	4	F5.0IV-V	Gra01
GJ 280 B	...	07 39 18.1	+05 13 30	.28517	.00064	4	DA	CNS91
GJ 1111	248	08 29 49.5	+26 46 37	.27580	.00300	1	M6.0V	Rei95
GJ 380	280	10 11 22.1	+49 27 15	.20553	.00049	2	K7.0V	Hen94
GJ 388	5167	10 19 36.4	+19 52 10	.20460	.00280	1	M3.0V	Hen94
LHS 288	288	10 44 21.2	-61 12 36	.20970	.00265	2	M5.5V	Hen04
LHS 292	292	10 48 12.6	-11 20 14	.22030	.00360	1	M6.5V	Rei95
DEN 1048-3956	...	10 48 14.6	-39 56 07	.24853	.00118	3	M8.5V	Hen04
GJ 406	36	10 56 29.2	+07 00 53	.41910	.00210	1	M6.0V	Hen94
GJ 411	37	11 03 20.2	+35 58 12	.39325	.00057	2	M2.0V	Hen94
GJ 412 A	38	11 05 28.6	+43 31 36	.20567	.00093	2	M1.0V	Hen94
GJ 412 B	39	11 05 30.4	+43 31 18	.20567	.00093	2	M5.5V	Hen94
GJ 440	43	11 45 42.9	-64 50 29	.21612	.00109	3	DQ6	CNS91
GJ 447	315	11 47 44.4	+00 48 16	.29814	.00137	2	M4.0V	Hen94
GJ 473 A	333	12 33 17.2	+09 01 15	.22790	.00460	1	M5.0V	Hen10
GJ 473 B	...	12 33 17.2	+09 01 15	.22790	.00460	1	M7.0V	CNS91
GJ 551	49	14 29 43.0	-62 40 46	.76885	.00029	4	M5.0V	CNS91
GJ 559 A	50	14 39 36.5	-60 50 02	.74723	.00117	1	G2.0V	Gra06
GJ 559 B	51	14 39 35.1	-60 50 14	.74723	.00117	1	K0.0V	CNS91
GJ 628	419	16 30 18.1	-12 39 45	.23438	.00150	2	M3.0V	Hen94
GJ 674	449	17 28 39.9	-46 53 43	.22011	.00139	2	M2.5V	Mon01
GJ 687	450	17 36 25.9	+68 20 21	.22047	.00083	2	M3.0V	Hen94
GJ 699	57	17 57 48.5	+04 41 36	.54551	.00029	2	M4.0V	Hen94
GJ 725 A	58	18 42 46.7	+59 37 49	.28383	.00146	3	M3.0V	Hen94
GJ 725 B	59	18 42 46.9	+59 37 37	.28383	.00146	3	M3.5V	Hen94
SCR 1845-6357 A	...	18 45 02.6	-63 57 52	.25950	.00111	2	M8.5V	Hen04

Table 1—Continued

Name	LHS	RA 2000.0	DEC	$\pi$	err	# of $\pi$	SpType	Ref
SCR 1845-6357 B	...	18 45 02.6	-63 57 52	.25950	.00111	2	T5.5V	Bil06
GJ 729	3414	18 49 49.4	-23 50 10	.33722	.00197	2	M3.5V	Hen10
GJ 1245 A	3494	19 53 54.2	+44 24 55	.22020	.00100	1	M5.5V	Hen94
GJ 1245 B	3495	19 53 55.2	+44 24 56	.22020	.00100	1	M6.0V	Hen94
GJ 1245 C	...	19 53 54.2	+44 24 55	.22020	.00100	1	M7.0V	Rei04
GJ 820 A	62	21 06 53.9	+38 44 58	.28608	.00048	3	K5.0V	Hen94
GJ 820 B	63	21 06 55.3	+38 44 31	.28608	.00048	3	K7.0V	Hen94
GJ 825	66	21 17 15.3	-38 52 03	.25344	.00080	2	M0.0V	Tor06
GJ 832	3685	21 33 34.0	-49 00 32	.20203	.00100	2	M1.5V	Joh10
GJ 845 A	67	22 03 21.7	-56 47 10	.27607	.00028	2	K4.0V	Gra06
GJ 845 B	...	22 04 10.5	-56 46 58	.27607	.00028	2	T1.0V	McC04
GJ 845 C	...	22 04 10.5	-56 46 58	.27607	.00028	2	T6.0V	McC04
GJ 860 A	3814	22 27 59.5	+57 41 45	.24806	.00139	2	M3.0V	Hen94
GJ 860 B	3815	22 27 59.5	+57 41 45	.24806	.00139	2	M4.0V	Hen94
GJ 866 A	68	22 38 33.4	-15 18 07	.28950	.00440	1	M5.0V	Hen02
GJ 866 B	...	22 38 33.4	-15 18 07	.28950	.00440	1	M	...
GJ 866 C	...	22 38 33.4	-15 18 07	.28950	.00440	1	M	...
GJ 876	530	22 53 16.7	-14 15 49	.21447	.00057	3	M4.0V	Mon01
GJ 887	70	23 05 52.0	-35 51 11	.30508	.00070	2	M2.0V	Tor06
GJ 905	549	23 41 55.0	+44 10 38	.31637	.00055	3	M5.5V	Hen94

Note. —

Bil06 Biller et al. (2006)  
CNS91 Catalog of Nearby Stars, Gliese & Jahreiss (1991)  
Cos06 Costa et al. (2006)  
Gra01 Gray et al. (2001)  
Gra06 Gray et al. (2006)  
Hen94 Henry et al. (1994)  
Hen02 Henry et al. (2002)  
Hen04 Henry et al. (2004)  
Hen06 Henry et al. (2006)  
Hen10 Henry et al. (2010)  
Jao08 Jao et al. (2008)  
Joh53 Johnson & Morgan (1953)  
Joh10 Johnson et al. (2010)  
McC04 McCaughrean et al. (2004)  
Mon01 Montes et al. (2001)  
Rei95 Reid et al. (1995)  
Rei04 Reid et al. (2004)  
Sch07 Schmidt et al. (2007)  
Tor06 Torres et al. (2006)  
YPC95 Yale Parallax Catalog, van Altena et al. (1995)

Table 2. Five Parsec Sample: Photometry

Name	U	Uref	B	Bref	V	Vref	R	Rref	I	Iref	J	err	H	err	K	err	Notes
Sum	-25.97	Alo95	-26.10	Alo95	-26.75	Alo95	-27.27	Alo95	-27.56	Alo95	-27.928	Alo95	-28.211	Alo95	-28.274	Alo95	...
GJ 1	...	...	10.02	Bes90	8.54	Bes90	7.57	Bes90	6.41	Bes90	5.328	0.019	4.828	0.076	4.523	0.017	...
GJ 1002	17.61	Leg92	15.73	Wei96	13.77	Bes91	12.16	Bes91	10.15	Bes91	8.323	0.019	7.792	0.034	7.439	0.021	...
GJ 15 A	10.87	Leg92	9.63	Leg92	8.08	Leg92	...	...	5.94	Leg92	5.252	0.264	4.476	0.200	4.018	0.020	...
GJ 15 B	14.26	Leg92	12.88	Wei96	11.06	Wei96	9.83	Wei96	8.24	Wei96	6.789	0.024	6.191	0.016	5.948	0.024	...
GJ 35	...	...	12.94	Bes90	12.40	Bes90	12.14	Bes90	11.91	Bes90	11.688	0.022	11.572	0.024	11.498	0.025	...
GJ 54.1	15.24	Leg92	13.95	Bes90	12.10	Bes90	10.73	Bes90	8.95	Bes90	7.258	0.020	6.749	0.033	6.420	0.017	...
GJ 65 A	14.96	Leg92	13.95	Bes90	12.61*	Hen99	10.40	Bes90	8.34	Bes90	6.86*	Hen93	6.30*	Hen93	5.91*	Hen93	joint UBRI
GJ 65 B	...	...	...	...	13.06*	Hen99	...	...	...	...	7.24*	Hen93	6.60*	Hen93	6.31*	Hen93	...
GJ 71	4.42	Joh66	4.21	Bes90	3.49	Bes90	3.06	Bes90	2.67	Bes90	2.06	Joh66	1.800	0.234	1.68	Joh66	...
GJ 83.1	15.47	Leg92	14.14	Bes90	12.31	Bes90	10.95	Bes90	9.21	Bes90	7.514	0.017	6.970	0.027	6.648	0.017	...
SO 0253+1652	...	...	...	...	15.13	Hen06	13.03	Hen06	10.65	Hen06	8.394	0.027	7.883	0.040	7.585	0.046	...
DEN 0255-4700	...	...	...	...	22.92	Cos06	19.90	Cos06	17.45	Cos06	13.246	0.027	12.204	0.024	11.558	0.024	...
GJ 144	...	...	4.61	Bes90	3.73	Bes90	3.22	Bes90	2.79	Bes90	2.20	Gla75	1.75	Gla75	1.65	Gla75	...
GJ 1061	...	...	...	...	13.09	Hen06	11.45	Hen06	9.46	Hen06	7.523	0.020	7.015	0.044	6.610	0.021	...
LP 944-020	...	...	...	...	...	...	...	...	13.29	Dea07	10.725	0.021	10.017	0.021	9.548	0.023	...
GJ 191	...	...	10.41	Bes90	8.85	Bes90	7.90	Bes90	6.90	Bes90	5.821	0.025	5.316	0.027	5.049	0.021	...
GJ 234 A	14.03	Leg92	12.81	Bes90	11.18*	Hen99	9.78	Bes90	8.08	Bes90	6.57*	Hen93	5.97*	Hen93	5.73*	Hen93	joint UBRI
GJ 234 B	...	...	...	...	14.26*	Hen99	...	...	...	...	8.36*	Hen93	7.60*	Hen93	7.23*	Hen93	...
GJ 244 AB	-1.4 1	Joh66	-1.43	Bes90	-1.43	Bes90	-1.42	Bes90	-1.41	Bes90	-1.391	0.109	-1.391	0.184	-1.390	0.214	joint
GJ 273	12.59	Wei93	11.42	Bes90	9.85	Bes90	8.70	Bes90	7.16	Bes90	5.032	0.032	5.219	0.063	4.857	0.022	...
GJ 280 AB	0.82	Joh66	0.79	Bes90	0.37	Bes90	0.12	Bes90	-0.12	Bes90	-0.40	Gla75	-0.60	Gla75	-0.65	Gla75	joint
GJ 1111	...	...	16.95	Bes90	14.90	Bes90	12.90	Bes90	10.64	Bes90	8.235	0.021	7.617	0.018	7.260	0.024	...
GJ 380	9.25	Leg92	7.97	Leg92	6.59	Leg92	5.74	Leg92	4.97	Leg92	3.98	Gla75	3.32	Gla75	3.19	Gla75	...
GJ 388	11.91	Leg92	10.85	Leg92	9.32	Leg92	8.23	Leg92	6.81	Leg92	5.449	0.027	4.843	0.020	4.593	0.017	...
LHS 288	...	...	...	...	13.92	Bes91	12.33	Bes91	10.31	Bes91	8.492	0.021	8.054	0.044	7.728	0.027	...
LHS 292	...	...	17.70	Leg92	15.73	Bes91	13.67	Bes91	11.33	Bes91	8.857	0.021	8.263	0.036	7.926	0.033	...
DEN 1048-3956	...	...	...	...	17.39	Jao05	15.05	Jao05	12.55	Jao05	9.538	0.022	8.905	0.044	8.447	0.023	...
GJ 406	17.03	Leg92	15.52	Bes90	13.53	Bes90	11.67	Bes90	9.50	Bes90	7.085	0.024	6.482	0.042	6.084	0.017	...
GJ 411	10.12	Leg92	8.98	Leg92	7.47	Leg92	6.46	Leg92	5.32	Leg92	4.13	Gla75	3.56	Gla75	3.20	Gla75	...
GJ 412 A	11.48	Leg92	10.34	Wei96	8.77	Wei96	7.79	Wei96	6.70	Wei96	5.538	0.019	5.002	0.021	4.769	0.020	...
GJ 412 B	...	...	16.53	Bes90	14.44	Bes90	12.77	Bes90	10.68	Bes90	8.742	0.025	8.177	0.024	7.839	0.026	...
GJ 440	11.04	Lan92	11.68	Lan92	11.50	Sub09	11.34	Sub09	11.20	Sub09	11.188	0.024	11.130	0.025	11.104	0.026	...
GJ 447	14.22	Leg92	12.92	Bes90	11.16	Bes90	9.85	Bes90	8.17	Bes90	6.505	0.023	5.945	0.024	5.654	0.024	...
GJ 473 A	...	...	15.06*	Tor99	13.25*	Tor99	...	...	...	...	7.69*	Tor99	7.06*	Tor99	6.59*	Tor99	...
GJ 473 B	...	...	15.11*	Tor99	13.24*	Tor99	...	...	...	...	7.82*	Tor99	7.26*	Tor99	7.03*	Tor99	...
GJ 551	14.36	Leg92	12.88	Bes90	11.05	Bes90	9.43	Bes90	7.43	Bes90	5.357	0.023	4.835	0.057	4.384	0.033	...
GJ 559 A	...	...	0.64	Bes90	0.01	Bes90	-0.35	Bes90	-0.68	Bes90	...	...	...	...	...	...	...
GJ 559 B	...	...	2.18	Bes90	1.34	Bes90	0.87	Bes90	0.46	Bes90	...	...	...	...	...	...	...
GJ 628	12.82	Wei93	11.68	Bes90	10.10	Bes90	8.94	Bes90	7.42	Bes90	5.950	0.024	5.373	0.040	5.075	0.024	...
GJ 674	...	...	10.90	Bes90	9.37	Bes90	8.30	Bes90	6.97	Bes90	5.711	0.019	5.154	0.033	4.855	0.018	...
GJ 687	11.76	Leg92	10.64	Wei96	9.17	Wei96	8.08	Wei96	6.68	Wei96	5.335	0.021	4.766	0.033	4.548	0.021	...
GJ 699	12.54	Leg92	11.31	Bes90	9.57	Bes90	8.35	Bes90	6.79	Bes90	5.244	0.020	4.834	0.034	4.524	0.020	...
GJ 725 A	11.55	Leg92	10.42	Wei96	8.90	Wei96	7.83	Wei96	6.48	Wei96	5.189	0.017	4.741	0.036	4.432	0.020	...
GJ 725 B	12.41	Leg92	11.28	Wei96	9.69	Wei96	8.57	Wei96	7.13	Wei96	5.721	0.020	5.197	0.024	5.000	0.022	...
SCR 1845-6357 AB	...	...	...	...	17.39	Hen06	14.99	Hen06	12.46	Hen06	9.544	0.023	8.967	0.027	8.508	0.020	joint
GJ 729	...	...	12.18	Bes90	10.44	Bes90	9.21	Bes90	7.65	Bes90	6.222	0.018	5.655	0.034	5.370	0.016	...
GJ 1245 A	...	...	15.31	Leg92	13.46*	Hen99	11.81	Wei96	9.78	Wei96	8.00*	Hen93	7.53*	Hen93	7.21*	Hen93	joint BRI
GJ 1245 C	...	...	...	...	16.75*	Hen99	...	...	...	...	9.35*	Hen93	8.61*	Hen93	8.24*	Hen93	...
GJ 1245 B	...	...	15.98	Leg92	14.01	Wei96	12.36	Wei96	10.27	Wei96	8.275	0.025	7.728	0.031	7.387	0.018	...
GJ 820 A	8.63	Joh66	7.40	Joh66	6.03	Joh66	4.86	Joh66	4.03	Joh66	3.114	0.268	2.540	0.198	2.248	0.318	...

Table 2—Continued

Name	U	Uref	B	Bref	V	Vref	R	Rref	I	Iref	J	err	H	err	K	err	Notes
GJ 820 B	8.62	Leg92	7.40	Leg92	6.03	Leg92	...	...	4.41	Leg92	3.546	0.278	2.895	0.218	2.544	0.328	...
GJ 825	9.29	Lei92	8.09	Bes90	6.67	Bes90	5.77	Bes90	4.91	Bes90	3.915	Mou76	3.270	Mou76	3.075	Mou76	...
GJ 832	11.36	Leg92	10.18	Bes90	8.66	Bes90	7.66	Bes90	6.47	Bes90	5.349	0.032	4.766	0.256	4.501	0.018	...
GJ 845 A	6.74	Joh66	5.73	Bes90	4.68	Bes90	4.06	Bes90	3.53	Bes90	2.894	0.292	2.349	0.214	2.237	0.240	...
GJ 845 BC	...	...	...	...	...	...	...	...	...	...	11.010	0.020	11.306	0.024	11.208	0.024	joint
GJ 860 A	...	...	...	...	9.86*	Hen93	...	...	...	...	5.91*	Hen93	5.33*	Hen93	5.02*	Hen93	...
GJ 860 B	...	...	...	...	11.41*	Hen93	...	...	...	...	7.10*	Hen93	6.47*	Hen93	6.39*	Hen93	...
GJ 866 AC	15.83	Leg92	14.33	Bes90	12.94*	Hen99	10.70	Bes90	8.64	Bes90	7.06*	Lei90	6.46*	Lei90	6.05*	Lei90	joint UBRI
GJ 866 B	...	...	...	...	13.34*	Hen99	...	...	...	...	7.62*	Lei90	7.02*	Lei90	6.61*	Lei90	...
GJ 876	12.90	Wei93	11.76	Bes90	10.18	Bes90	9.00	Bes90	7.43	Bes90	5.934	0.019	5.349	0.049	5.010	0.021	...
GJ 887	...	...	8.84	Bes90	7.34	Bes90	6.37	Bes90	5.32	Bes90	4.338	0.258	3.608	0.230	3.465	0.200	...
GJ 905	15.65	Leg92	14.20	Wei96	12.29	Wei96	10.77	Wei96	8.82	Wei96	6.884	0.025	6.247	0.027	5.929	0.020	...
GJ 166 A	...	...	...	...	4.43	Bes90	3.96	Bes90	3.54	Bes90	3.013	0.238	2.594	0.198	2.498	0.236	...
GJ 166 B	8.88	Kid91	9.56	Kid91	9.53	Kid91	...	...	...	...	9.849	0.029	9.986	0.039	9.861	0.071	...
GJ 166 C	...	...	12.84	Rei04	11.17	Rei04	...	...	...	...	6.747	0.020	6.278	0.040	5.962	0.026	...

Note. — JHK & err from 2MASS unless otherwise noted.

\* deconvolved using flux ratios from references given and available optical and infrared photometry

“joint” indicates unresolved photometry.

Alo95 Alonso et al. (1995)

Bes90 Bessell (1990)

Bes91 Bessell (1991)

Cos06 Costa et al. (2006)

Dea07 Deacon & Hambly (2007)

Gla75 Glass (1975)

Hen93 Henry & McCarthy (1993)

Hen99 Henry et al. (1999)

Hen06 Henry et al. (2006)

Jao05 Jao et al. (2005)

Joh66 Johnson et al. (1966)

Kid91 Kidder et al. (1991)

Lan92 Landolt (1992)

Leg92 Leggett (1992)

Lei90 Leinert et al. (1990)

Mou76 Mould & Hyland (1976)

Sub09 Subasavage et al. (2009)

Wei93 Weis (1993)

Wei96 Weis (1996)

Tor99 Torres et al. (1999)

Table 3. Extended Ten Parsec Sample

Name	LHS	RA 2000.0	DEC	$\pi$	err	# of $\pi$	SpType	Ref
GJ 17	5	00 20 04.2	-64 52 29	.11647	.00016	2	F9.5V	Gra06
GJ 19	6	00 25 45.1	-77 15 15	.13407	.00011	2	G0.0V	Gra06
GJ 33	121	00 48 23.0	+05 16 50	.13426	.00049	2	K2.5V	Gra06
GJ 34 A	123	00 49 06.3	+57 48 55	.16823	.00046	2	G3.0V	Mon01
GJ 53 A	8	01 08 16.4	+54 55 13	.13267	.00074	2	G5.0V	Joh53
GJ 66 A	...	01 39 47.6	-56 11 47	.12999	.00208	2	K5.0V	Mon01
GJ 66 B	...	01 39 47.6	-56 11 36	.12999	.00208	2	K5.0V	Mon01
GJ 68	1287	01 42 29.8	+20 16 07	.13275	.00049	2	K1.0V	Gra06
GJ 105 A	15	02 36 04.9	+06 53 13	.13906	.00044	2	K3.0V	Gra06
GJ 139	19	03 19 55.7	-43 04 11	.16547	.00019	2	G8.0V	Pas94
GJ 150	1581	03 43 14.9	-09 45 48	.11063	.00022	2	K1.0III-IV	Gra06
GJ 178	...	04 49 50.4	+06 57 41	.12393	.00017	2	F6.0V	Mon01
GJ 183	200	05 00 49.0	-05 45 13	.11477	.00048	2	K3.0V	CNS91
GJ 216 A	...	05 44 27.8	-22 26 54	.11204	.00018	2	F6.0V	Mon01
GJ 216 B	...	05 44 26.5	-22 25 19	.11204	.00018	2	K2.0V	CNS91
GJ 222 A	...	05 54 23.0	+20 16 34	.11522	.00025	3	G0.0V	CNS91
GJ 250 A	1875	06 52 18.1	-05 10 25	.11465	.00043	2	K3.0V	CNS91
GJ 423 A	2390	11 18 10.9	+31 31 45	.11951	.00079	2	G0.0V	Bat89
GJ 423 B	2391	11 18 11.0	+31 31 46	.11951	.00079	2	G5.0V	Bat89
GJ 432 A	308	11 34 29.5	-32 49 53	.10461	.00037	2	K0.0V	CNS91
GJ 434	...	11 41 03.0	+34 12 06	.10416	.00026	2	G8.0V	CNS91
GJ 442 A	311	11 46 31.1	-40 30 01	.10844	.00022	2	G2.0V	Gra06
GJ 451	44	11 52 58.8	+37 43 07	.11013	.00040	2	G8.0V	Joh53
GJ 475	2579	12 33 44.5	+41 21 27	.11848	.00020	2	G0.0V	CNS91
GJ 502	348	13 11 52.4	+27 52 41	.10952	.00017	2	G0.0V	CNS91
GJ 506	349	13 18 24.3	-18 18 40	.11690	.00022	2	G7.0V	Gra06
GJ 566 A	...	14 51 23.4	+19 06 02	.14757	.00072	2	G8.0V	Ruc95
GJ 566 B	...	14 51 23.4	+19 06 02	.14757	.00072	2	K4.0V	Mon99
GJ 570 A	387	14 57 28.0	-21 24 56	.17062	.00067	3	K4.0V	Gra06
GJ 631	3224	16 36 21.4	-02 19 29	.10249	.00040	2	K2.0V	Mon01
GJ 638	...	16 45 06.4	+33 30 33	.10195	.00070	2	K7.0V	CNS91
GJ 663 A	437	17 15 20.9	-26 36 09	.16812	.00040	4	K1.0V	CNS91
GJ 663 B	438	17 15 21.0	-26 36 10	.16812	.00040	4	K1.0V	CNS91
GJ 664(C)*	439	17 16 13.4	-26 32 46	.16812	.00040	4	K5.0V	CNS91
GJ 667 A	442	17 18 57.2	-34 59 23	.13822	.00070	2	K3.0V	CNS91
GJ 667 B	443	17 19 01.9	-34 59 33	.13822	.00070	2	K5.0V	CNS91
GJ 666 A	444	17 19 03.8	-46 38 10	.11371	.00069	2	G8.0V	CNS91
GJ 673	447	17 25 45.2	+02 06 41	.12987	.00071	2	K7.0V	CNS91
GJ 695 A	3326	17 46 27.5	+27 43 14	.12032	.00016	2	G5.0IV	CNS91
GJ 702 A	458	18 05 27.4	+02 29 59	.19596	.00087	2	K0.0V	CNS91
GJ 702 B	459	18 05 27.4	+02 29 56	.19596	.00087	2	K5.0V	CNS91
GJ 713 A	3379	18 21 03.4	+72 43 58	.12343	.00044	3	F7.0V	CNS91
GJ 713 B	...	18 21 03.4	+72 43 58	.12343	.00044	3	G8.0V	Far10
GJ 721	...	18 36 56.3	+38 47 01	.12985	.00032	3	A0.0V	CNS91
GJ 764	447	19 32 21.6	+69 39 40	.17379	.00018	2	K0.0V	CNS91
GJ 768	3490	19 50 47.0	+08 52 06	.19540	.00046	3	A7.0V	CNS91
GJ 780	485	20 08 43.6	-66 10 55	.16371	.00017	2	G8.0IV	Gra06
GJ 783 A	486	20 11 11.9	-36 06 04	.16626	.00027	2	K2.5V	Gra06
GJ 785	488	20 15 17.4	-27 01 59	.11222	.00030	2	K2.0V	Gra06
GJ 827	3674	21 26 26.6	-65 21 58	.10797	.00019	2	F9.0V	Gra06
GJ 881(A)	...	22 57 39.0	-29 37 20	.13042	.00037	4	A4.0V	Gra06

Table 3—Continued

Name	LHS	RA 2000.0	DEC	$\pi$	err	# of $\pi$	SpType	Ref
GJ 879(B)*	...	22 56 24.1	-31 33 56	.13042	.00037	4	K5.0V	CNS91
GJ 884	3885	23 00 16.1	-22 31 28	.12175	.00069	2	K7.0V	Gra06
GJ 892	71	23 13 17.0	+57 10 06	.15284	.00028	2	K3.0V	CNS91

Note. — \* Designates component to above system with different GJ number.  
 Bat89 Batten et al. (1989)  
 CNS91 Catalog of Nearby Stars, Gliese & Jahreiss (1991)  
 Far10 Farrington et al. (2010)  
 Gra06 Gray et al. (2006)  
 Mon99 Montes et al. (1999)  
 Mon01 Montes et al. (2001)  
 Pas94 Pasquini et al. (1994)  
 Ruc95 Ruck & Smith (1995)  
 Joh53 Johnson & Morgan (1953)

Table 4. Extended Ten Parsec Sample: Photometry

Name	U	Uref	B	Bref	V	Vref	R	Rref	I	Iref	J	err	H	err	K	err	Notes
GJ 17	4.82	Joh66	4.80	Bes90	4.22	Bes90	3.89	Bes90	3.57	Bes90	3.17	Gla75	2.87	Gla75	2.78	Gla75	...
GJ 19	3.53	Joh66	3.42	Bes90	2.80	Bes90	2.45	Bes90	2.12	Bes90	1.72	Gla75	1.40	Gla75	1.32	Gla75	...
GJ 33	...	...	6.60	Bes90	5.72	Bes90	5.21	Bes90	4.76	Bes90	4.24	Joh68	3.72	Joh68	3.48	Joh68	...
GJ 34 A	4.04	Joh66	4.02	Joh66	3.44	Joh66	3.1	USNOB	2.8	USNOB	2.109	0.570	2.086	0.504	1.988	...	...
GJ 53 AB	5.96	Joh66	5.87	Joh66	5.18	Joh66	4.7	USNOB	4.4	USNOB	3.86	Joh68	3.39	Joh68	3.36	Joh68	joint
GJ 66 A	...	...	6.69	Hog00	5.80	Hog00	...	...	...	...	4.043	0.378	...	...	3.510	0.282	...
GJ 66 B	...	...	6.84	Mer86	5.96	Mer86	...	...	...	...	3.573	...	...	...	3.558	0.270	...
GJ 68	6.57	Joh66	6.08	Joh66	5.24	Joh66	4.7	USNOB	4.3	USNOB	3.855	0.24	3.391	0.226	3.285	0.266	...
GJ 105 AC	...	...	6.78	Bes90	5.81	Bes90	5.24	Bes90	4.74	Bes90	4.07	Gla75	3.52	Gla75	3.45	Gla75	joint
GJ 139	5.19	Joh66	4.97	Bes90	4.26	Bes90	3.85	Bes90	3.47	Bes90	2.95	Gla75	2.59	Gla75	2.52	Gla75	...
GJ 150	...	...	4.45	Bes90	3.53	Bes90	3.03	Bes90	2.59	Bes90	1.99	Gla75	1.53	Gla75	1.45	Gla75	...
GJ 178	3.64	Joh66	3.65	Bes90	3.19	Bes90	2.92	Bes90	2.67	Bes90	2.35	Gla75	2.15	Gla75	2.07	Gla75	...
GJ 183	...	...	7.29	Bes90	6.23	Bes90	5.44	Bes90	4.69	Bes90	4.389	0.244	3.797	0.214	3.706	0.228	...
GJ 216 A	4.07	Joh66	4.06	Bes90	3.59	Bes90	3.30	Bes90	3.02	Bes90	2.804	0.276	2.606	0.236	2.508	0.228	...
GJ 216 B	...	...	7.12	Bes90	6.18	Bes90	5.63	Bes90	5.17	Bes90	4.845	0.198	4.158	0.202	4.131	0.264	...
GJ 222 AB	5.04	Joh66	5.00	Joh66	4.41	Joh66	4.0	USNOB	3.8	USNOB	3.34	Joh68	3.04	Joh68	2.97	Joh68	joint
GJ 250 A	...	...	7.64	Bes90	6.59	Bes90	5.98	Bes90	5.45	Bes90	5.013	0.252	4.294	0.258	4.107	0.036	...
GJ 423 AC	...	...	4.78	Lep05	4.27	Lep05	3.9	USNOB	3.7	USNOB	2.462	0.294	2.231	0.204	2.142	0.230	joint
GJ 423 BD	...	...	5.36	Lep05	4.74	Lep05	4.4	USNOB	4.0	USNOB	...	...	...	...	...	...	joint
GJ 432 A	...	...	6.78	Bes90	5.97	Bes90	5.52	Bes90	5.10	Bes90	4.784	0.228	4.138	0.214	4.022	0.036	...
GJ 434	6.28	Joh66	6.05	Bes90	5.33	Bes90	4.9	USNOB	4.5	USNOB	3.99	Joh68	3.61	Joh68	3.60	Joh68	...
GJ 442 A	...	...	5.56	Bes90	4.90	Bes90	4.5	USNOB	4.2	USNOB	3.931	0.276	3.490	0.238	3.489	0.278	...
GJ 451	7.37	Joh66	7.20	Joh66	6.45	Joh66	6.0	USNOB	5.6	USNOB	4.89	Gla75	4.43	Gla75	4.37	Gla75	...
GJ 475	4.91	Joh66	4.86	Joh66	4.27	Joh66	3.9	USNOB	3.6	USNOB	3.23	Joh66	2.905	0.198	2.84	Joh66	...
GJ 502	4.92	Joh66	4.84	Joh66	4.26	Joh66	3.9	USNOB	3.6	USNOB	3.24	Gla75	2.90	Gla75	2.87	Gla75	...
GJ 506	5.69	Joh66	5.43	Bes90	4.72	Bes90	4.33	Bes90	3.97	Bes90	3.334	0.200	2.974	0.176	2.956	0.236	...
GJ 566 A	5.68	Lut71	5.44	Lut71	4.72	Lut71	4.52	Bre64	4.24	Bre64	2.660	0.448	2.253	0.698	1.971	0.600	joint JHK
GJ 566 B	9.29	Lut71	8.14	Lut71	6.97	Lut71	6.30	Bre64	5.86	Bre64	...	...	...	...	...	...	...
GJ 570 A	7.88	Joh66	6.82	Joh66	5.71	Joh66	...	...	...	...	3.663	0.258	3.085	0.196	3.048	0.224	...
GJ 631	...	...	6.57	Bes90	5.76	Bes90	5.31	Bes90	4.9	Bes90	4.33	Joh66	4.053	0.208	3.87	Joh66	...
GJ 638	...	...	9.48	Joh53	8.11	Joh65	7.3	USNOB	6.6	USNOB	5.48	0.023	4.878	0.018	4.712	0.021	...
GJ 663 AB	...	...	5.93	Tor06	5.08	Tor06	...	...	...	...	...	...	...	...	...	...	joint
GJ 664(C)*	...	...	7.48	Bes90	6.32	Bes90	5.62	Bes90	5.04	Bes90	4.155	0.25	...	...	3.466	0.256	...
GJ 667 AB	7.77	Joh66	6.95	Joh66	5.91	Joh66	4.97	Joh66	4.38	Joh66	3.903	0.262	3.230	0.206	3.123	0.278	joint
GJ 666 A	...	...	6.35	Bes90	5.47	Bes90	5.00	Bes90	4.54	Bes90	4.077	0.996	3.146	0.664	3.421	0.282	...
GJ 673	...	...	8.89	Bes90	7.53	Bes90	6.69	Bes90	5.94	Bes90	4.934	0.024	4.341	0.044	4.14	Gla75	...
GJ 695 AD	4.56	Joh66	4.17	Joh66	3.42	Joh66	2.9	USNOB	2.6	USNOB	2.13	Joh66	1.559	0.184	1.77	Joh66	joint
GJ 702 A	5.31	Egg65	4.98	Egg65	4.20	Egg65	3.87	Bre64	3.61	Bre64	2.343	0.296	1.876	0.244	1.791	0.304	joint JHK
GJ 702 B	...	...	7.15	Egg65	6.00	Egg65	5.26	Bre64	4.82	Bre64	...	...	...	...	...	...	...
GJ 713 AB	4.01	Joh66	4.07	Joh66	3.58	Joh66	3.3	USNOB	3.0	USNOB	2.588	0.260	2.372	0.188	2.216	0.252	joint
GJ 721	0.02	Joh66	0.02	Bes90	0.03	Bes90	0.04	Bes90	0.04	Bes90	0.02	Joh66	-0.029	0.146	0.02	Joh66	...
GJ 764	5.86	Oja84	5.46	Oja93	4.68	Oja93	4.2	USNOB	3.8	USNOB	3.32	Joh66	3.039	0.214	2.78	Joh66	...
GJ 768	1.07	Joh66	0.99	Bes90	0.77	Bes90	0.64	Bes90	0.50	Bes90	0.39	Joh66	0.102	0.220	0.26	Joh66	...
GJ 780	4.76	Joh66	4.31	Bes90	3.55	Bes90	3.14	Bes90	2.79	Bes90	2.35	Gla75	2.03	Gla75	1.93	Gla75	...
GJ 783 A	...	...	6.19	Joh66	5.32	Joh66	...	...	...	...	3.518	0.300	2.999	0.422	3.008	0.602	...
GJ 785	...	...	6.61	Bes90	5.73	Bes90	5.23	Bes90	4.81	Bes90	4.112	0.294	3.582	0.266	3.501	0.232	...
GJ 827	4.58	Joh66	4.71	Bes90	4.22	Bes90	3.92	Bes90	3.61	Bes90	3.27	Gla75	3.00	Gla75	2.90	Gla75	...
GJ 881(A)	1.30	Joh66	1.24	Bes90	1.15	Bes90	1.10	Bes90	1.07	Bes90	1.02	Gla75	1.03	Gla75	0.99	Gla75	...
GJ 879(B)*	...	...	7.56	Bes90	6.46	Bes90	5.8	Bes90	5.78	Bes90	4.533	0.037	3.804	0.210	3.805	0.240	...
GJ 884	...	...	9.25	Bes90	7.86	Bes90	7.00	Bes90	6.23	Bes90	5.346	0.021	4.696	0.076	4.478	0.016	...
GJ 892	7.46	Oja84	6.56	Oja93	5.57	Oja93	4.9	USNOB	4.5	USNOB	3.80	Gla75	3.27	Gla75	3.18	Gla75	...

Table 4—Continued

Name	U	Uref	B	Bref	V	Vref	R	Rref	I	Iref	J	err	H	err	K	err	Notes
------	---	------	---	------	---	------	---	------	---	------	---	-----	---	-----	---	-----	-------

Note. — \* Designates component to above system with different GJ number.  
 JHK & err from 2MASS unless otherwise noted.  
 “joint” indicates unresolved photometry.  
 Bes90 Bessell (1990)  
 Bre64 Breckinridge & Kron (1964)  
 Egg65 Eggen (1965)  
 Gla75 Glass (1975)  
 Hog00 Høg et al. (2000)  
 Joh53 Johnson & Morgan (1953)  
 Joh66 Johnson et al. (1966)  
 Joh68 Johnson et al. (1968)  
 Lep05 Lépine & Shara (2005)  
 Lut71 Lutz (1971)  
 Mer86 Mermilliod (1986)  
 Oja84 Oja (1984)  
 Oja93 Oja (1993)  
 Tor06 Torres et al. (2006)  
 USNOB Monet et al. (2003)



Table 5. *UBVRIJK* Zero Points

Filter	Zero Point	$\lambda_{eff}(\text{\AA})$	Ref
U	4.18e-9	3660	Bessell et al.(1998)
B	6.32e-9	4380	Bessell et al.(1998)
V	3.63e-9	5450	Bessell et al.(1998)
R	2.18e-9	6410	Bessell et al.(1998)
I	1.13e-9	7980	Bessell et al.(1998)
J	3.14e-10	12350	Cohen et al.(2003)
H	1.11e-10	16620	Cohen et al.(2003)
K	4.29e-11	21590	Cohen et al.(2003)

Note. — Zero points have units of  $\text{ergs cm}^2 \text{sec}^{-1} \text{\AA}^{-1}$ .

Table 6. Comparison of Derived Temperatures and Radii for Nearby Stars Using Our SED Fits and Interferometric Results

Star	SpType	V-K	$T_{\text{eff}}^{\text{Model}}$	$T_{\text{eff}}^{\text{ModelFixR}}$	$T_{\text{eff}}^{\text{Published}}$	$R/R_{\odot}^{\text{Model}}$	$R/R_{\odot}^{\text{Pub}}$	Ref.
GJ 244 A	A1.0V	-0.040	10000	9600	9900±200	1.645	1.711± 0.013	Kervella et al (2003a)
GJ 280 A	F5.0IV-V	1.028	6700	6500	6524	1.898	2.048± 0.025	Kervella et al (2003b)
GJ 559 A	G2.0V	1.490	6000	5700	5810±50	1.103	1.224± 0.003	Kervella et al (2003b)
GJ 71	G8.5V	1.696	5700	5400	5264±100	0.708	0.816± 0.013	Di Folco et al.(2004)
GJ 631	K2.0V	1.890	5500	5300	5337±41	0.710	0.759± 0.012	Boyajian et al.(2012)
GJ 166 A	K0.5V	1.932	5200	5100	5143±14	0.735	0.806± 0.004	Boyajian et al.(2012)
GJ 559 B	K0.0V	1.940	5400	5100	5260±50	0.775	0.863± 0.005	Kervella et al (2003b)
GJ 144	K2.0V	1.954	5200	5000	5135±100	0.689	0.743± 0.005	Di Folco et al.(2004)
GJ 33	K2.5V	2.240	5200	5000	4950±14	0.643	0.695± 0.004	Boyajian et al.(2012)
GJ 105 A	K3.0V	2.360	5000	4700	4662±17	0.677	0.795± 0.006	Boyajian et al.(2012)
GJ 892	K3.0V	2.390	5000	4800	4699±16	0.698	0.778± 0.005	Boyajian et al.(2012)
GJ 702 A	K0.0V	2.409	5500	5700	5407±52	0.754	0.831± 0.004	Boyajian et al.(2012)
GJ 845 A	K5.0V	2.443	4900	4600	5468±59	0.608	0.732± 0.007	Demory et al.(2009)
GJ 570 A	K4.0V	2.662	4700	4700	4507±58	0.734	0.739± 0.019	Boyajian et al.(2012)
GJ 820 B	K7.0V	3.486	4300	4200	4040±80	0.530	0.595± 0.008	Kervella et al (2008)
GJ 380	K7.0V	3.628	4200	4200	4081±15	0.599	0.642± 0.005	Boyajian et al.(2012)
GJ 820 A	K5.0V	3.782	4000	4100	4400±100	0.709	0.665± 0.005	Kervella et al (2008)
GJ 702 B*	K5.0V	...	...	...	4393±149	...	0.670± 0.009	Boyajian et al.(2012)
GJ 191	M2.0VI	3.801	3800	3600	3570±156	0.249	0.291± 0.025	Ségransan et al.(2003)
GJ 887	M2.0V	3.875	3800	3700	3797±45	0.414	0.459± 0.011	Demory et al.(2009)
GJ 411	M2.0V	3.969	3700	3500	3465±17	0.338	0.392± 0.004	Boyajian et al.(2012)
GJ 412 A	M1.0V	4.001	3700	3600	3497±39	0.353	0.398± 0.009	Boyajian et al.(2012)
GJ 15 A	M1.5V	4.062	3800	3700	3730±49	0.323	0.379± 0.006	Berger et al. (2006)
GJ 725 A	M3.0V	4.468	3400	3400	3407±15	0.344	0.356± 0.004	Boyajian et al.(2012)
GJ 687	M3.0V	4.622	3400	3200	3413±28	0.406	0.418± 0.007	Boyajian et al.(2012)
GJ 725 B	M3.5V	4.690	3300	3200	3104±28	0.275	0.323± 0.006	Boyajian et al.(2012)
GJ 699	M4.0V	5.046	3100	3100	3224±10	0.198	0.187± 0.001	Boyajian et al.(2012)
GJ 551	M5.0V	6.666	2700	2900	3098±56	0.167	0.141± 0.007	Demory et al.(2009)

Note. —  $T_{\text{eff}}^{\text{Model}}$  refers to temperatures from our model, while,  $T_{\text{eff}}^{\text{ModelFixR}}$  refers to temperatures derived while holding the radius to values obtained through long baseline interferometry.

\* GJ 702B does not have enough resolved photometry for a model solution.

Table 7. Empirical Habitable Zones (EHZs) for the Five Parsec Sample

Name	SpType	Model					Model FixR				
		R ( $R/R_{\odot}$ )	$T_{\text{eff}}$ (K)	EHZ Inner R (AU)	EHZ Outer R (AU)	EHZ Lin (AU)	R ( $R/R_{\odot}$ )	$T_{\text{eff}}$ (K)	EHZ Inner R (AU)	EHZ Outer R (AU)	EHZ Lin (AU)
Sun	G2.0V	0.917	6000	0.789	1.686	0.897	1.00	5800	0.804	1.718	0.914
DEN 1048-3956	M8.5V	0.134	2000	0.013	0.027	0.014	...	...	...	...	...
GJ 1	M1.5V	0.349	3700	0.114	0.244	0.130	...	...	...	...	...
GJ 15 A	M1.5V	0.323	3800	0.112	0.239	0.127	0.387	3700	0.127	0.271	0.144
GJ 15 B	M3.5V	0.197	3200	0.048	0.103	0.055	...	...	...	...	...
GJ 54.1	M4.5V	0.181	2900	0.036	0.078	0.042	...	...	...	...	...
GJ 65 A	M5.5V	0.248	2600	0.040	0.086	0.046	...	...	...	...	...
GJ 65 B	M6.0V	0.225	2700	0.039	0.084	0.045	...	...	...	...	...
GJ 71	G8.0V	0.700	5700	0.545	1.164	0.619	0.816	5400	0.570	1.218	0.648
GJ 83.1	M4.5V	0.195	2900	0.039	0.084	0.045	...	...	...	...	...
GJ 144	K2.0V	0.630	5400	0.440	0.940	0.500	0.735	5000	0.440	0.941	0.500
GJ 166 A	K0.5V	0.735	5200	0.476	1.017	0.541	0.806	5000	0.483	1.031	0.549
GJ 166 C	M4.5V	0.249	3200	0.061	0.130	0.069	...	...	...	...	...
GJ 191	M1.5VI	0.240	3800	0.083	0.177	0.094	0.291	3500	0.085	0.182	0.097
GJ 234 A	M4.0V	0.287	3000	0.062	0.132	0.070	...	...	...	...	...
GJ 234 B	M5.5V	0.155	2700	0.027	0.058	0.031	...	...	...	...	...
GJ 244 A*	A1.0V	1.645	10000	3.942	8.420	4.478	1.711	9600	3.779	8.071	4.293
GJ 273	M3.5V	0.316	3200	0.077	0.165	0.088	...	...	...	...	...
GJ 280 A*	F5.0IV-V	1.906	6700	2.050	4.380	2.329	2.048	6500	2.073	4.429	2.356
GJ 380	K7.0V	0.648	4100	0.261	0.558	0.297	0.642	4100	0.259	0.552	0.294
GJ 388	M3.0V	0.452	3300	0.118	0.251	0.133	...	...	...	...	...
GJ 406	M6.0V	0.162	2500	0.024	0.052	0.028	...	...	...	...	...
GJ 411	M2.0V	0.338	3700	0.111	0.237	0.126	0.392	3500	0.115	0.246	0.130
GJ 412 A	M1.0V	0.353	3700	0.116	0.247	0.131	0.398	3600	0.124	0.264	0.140
GJ 412 B	M5.5V	0.152	2600	0.025	0.053	0.028	...	...	...	...	...
GJ 447	M4.0V	0.213	3000	0.046	0.098	0.052	...	...	...	...	...
GJ 473 A	M5.0V	0.212	2700	0.037	0.079	0.042	...	...	...	...	...
GJ 473 B	M7.0V	0.177	2900	0.036	0.076	0.040	...	...	...	...	...
GJ 551	M5.5V	0.167	2700	0.029	0.062	0.033	0.141	2900	0.028	0.061	0.032
GJ 559 A	G2.0V	0.884	6700	0.951	2.031	1.080	1.224	5700	0.953	2.036	1.083
GJ 559 B	K0.0V	0.774	5400	0.541	1.155	0.614	0.863	5200	0.559	1.194	0.635
GJ 628	M3.0V	0.321	3200	0.079	0.168	0.089	...	...	...	...	...

Table 7—Continued

Name	SpType	Model					Model FixR				
		R ( $R/R_{\odot}$ )	$T_{\text{eff}}$ (K)	EHZ Inner R (AU)	EHZ Outer R (AU)	EHZ Lin (AU)	R ( $R/R_{\odot}$ )	$T_{\text{eff}}$ (K)	EHZ Inner R (AU)	EHZ Outer R (AU)	EHZ Lin (AU)
GJ 674	M2.5V	0.355	3400	0.098	0.210	0.112	...	...	...	...	...
GJ 687	M3.0V	0.406	3400	0.112	0.240	0.128	0.418	3400	0.116	0.247	0.132
GJ 699	M4.0V	0.198	3100	0.046	0.097	0.051	0.187	3100	0.043	0.092	0.048
GJ 725 A	M3.0V	0.344	3400	0.095	0.204	0.109	0.356	3400	0.099	0.211	0.112
GJ 725 B	M3.5V	0.275	3300	0.072	0.153	0.081	0.323	3200	0.079	0.169	0.090
GJ 729	M3.5V	0.214	3100	0.049	0.105	0.056	...	...	...	...	...
GJ 820 A	K5.0V	0.709	4000	0.272	0.581	0.309	0.665	4100	0.268	0.572	0.304
GJ 820 B	K7.0V	0.530	4300	0.235	0.502	0.267	0.595	4200	0.252	0.537	0.286
GJ 825	M0.0V	0.516	4100	0.208	0.444	0.236	...	...	...	...	...
GJ 832	M1.5V	0.423	3600	0.131	0.280	0.149	...	...	...	...	...
GJ 845 A	K5.0V	0.608	4900	0.350	0.747	0.397	0.732	4600	0.371	0.793	0.422
GJ 860 A	M3.0V	0.328	3300	0.085	0.183	0.098	...	...	...	...	...
GJ 860 B	M4.0V	0.194	3200	0.048	0.102	0.054	...	...	...	...	...
GJ 866 B	MV	0.215	2700	0.037	0.080	0.043	...	...	...	...	...
GJ 876 A	M4.0V	0.390	3100	0.090	0.191	0.101	...	...	...	...	...
GJ 887	M1.5V	0.414	3800	0.143	0.306	0.163	0.491	3700	0.161	0.344	0.183
GJ 905	M5.5V	0.216	2700	0.038	0.080	0.042	...	...	...	...	...
GJ 1002	M5.0V	0.142	2900	0.029	0.061	0.032	...	...	...	...	...
GJ 1061	M5.0V	0.178	2700	0.031	0.066	0.035	...	...	...	...	...
GJ 1111	M6.0V	0.162	2400	0.022	0.048	0.026	...	...	...	...	...
GJ 1245 A	M5.5V	0.194	2700	0.034	0.072	0.038	...	...	...	...	...
GJ 1245 B	M6.0V	0.150	2700	0.026	0.056	0.030	...	...	...	...	...
GJ 1245 C	M7.0V	0.171	2100	0.018	0.039	0.021	...	...	...	...	...
LHS 288	M5.5V	0.150	2700	0.026	0.056	0.030	...	...	...	...	...
LHS 292	M6.5V	0.146	2400	0.020	0.043	0.023	...	...	...	...	...
LP 944-020	M9.0V	0.091	2000	0.009	0.019	0.010	...	...	...	...	...
SCR 1845-6357 A	M8.5V	0.129	2000	0.012	0.026	0.014	...	...	...	...	...
SO 0253+1652	M7.0V	0.156	2400	0.022	0.046	0.024	...	...	...	...	...

Note. — This table shows model radius, temperature, inner and outer HZ radius, and the HZ width in AU in columns 3-7. Columns 8-12 show radius, temperature, inner and outer HZ radius, and the HZ width in AU based on the method of holding the stellar radius to the values obtained through long baseline interferometry (see

Table 6). \* Sirius (GJ 244A) and Procyon (GJ 280A) are included as benchmarks, but are not used in final EHZ calculations because of companion white dwarfs.

Table 8. Empirical Habitable Zones (EHZs) for the Extended Ten Parsec Sample

Name	SpType	Model					Model FixR				
		R ( $R/R_{\odot}$ )	$T_{\text{eff}}$ (K)	EHZ Inner R (AU)	EHZ Outer R (AU)	EHZ Lin (AU)	R ( $R/R_{\odot}$ )	$T_{\text{eff}}$ (K)	EHZ Inner R (AU)	EHZ Outer R (AU)	EHZ Lin (AU)
GJ 17	F9.5V	0.989	6100	0.882	1.884	1.002	...	...	...	...	...
GJ 19	G0.0V	1.709	6000	1.474	3.149	1.675	...	...	...	...	...
GJ 33	K2.5V	0.643	5200	0.417	0.890	0.473	0.695	5000	0.416	0.889	0.473
GJ 34 A	G3.0V	0.989	6100	0.882	1.884	1.002	...	...	...	...	...
GJ 66 A	K5.0V	0.740	5100	0.461	0.985	0.524	...	...	...	...	...
GJ 66 B	K5.0V	0.794	4900	0.457	0.976	0.519	...	...	...	...	...
GJ 68	K1.0V	0.739	5400	0.516	1.103	0.587	...	...	...	...	...
GJ 105 A	K3.0V	0.677	5000	0.406	0.866	0.460	0.795	4700	0.421	0.899	0.478
GJ 139	G8.0V	0.812	5700	0.632	1.350	0.718	...	...	...	...	...
GJ 178	F6.0V	1.244	6600	1.299	2.774	1.475	...	...	...	...	...
GJ 183	K3.0V	0.791	4800	0.437	0.933	0.496	...	...	...	...	...
GJ 216 A	F6.0V	1.137	6600	1.187	2.534	1.347	...	...	...	...	...
GJ 216 B	K2.0V	0.593	5300	0.399	0.853	0.454	...	...	...	...	...
GJ 250 A	K3.0V	0.597	4900	0.344	0.734	0.390	...	...	...	...	...
GJ 432 A	K0.0V	0.627	5500	0.455	0.971	0.516	...	...	...	...	...
GJ 434	G8.0V	0.793	5700	0.617	1.319	0.702	...	...	...	...	...
GJ 442 A	G2.0V	0.792	6000	0.683	1.459	0.776	...	...	...	...	...
GJ 451	G8.0V	0.542	5400	0.378	0.807	0.429	...	...	...	...	...
GJ 475	G0.0V	0.952	6100	0.849	1.813	0.964	...	...	...	...	...
GJ 502	G0.0V	1.029	6100	0.918	1.960	1.042	...	...	...	...	...
GJ 506	G7.0V	0.927	5700	0.722	1.542	0.820	...	...	...	...	...
GJ 566 A	G8.0V	0.534	6200	0.491	1.049	0.558	...	...	...	...	...
GJ 566 B	K4.0V	0.376	5000	0.225	0.481	0.256	...	...	...	...	...
GJ 570 A	K4.0V	0.734	4700	0.389	0.830	0.441	0.739	4700	0.391	0.836	0.444
GJ 631	K2.0V	0.710	5500	0.515	1.099	0.584	0.759	5300	0.511	1.091	0.580
GJ 638	K7.0V	0.620	4100	0.250	0.534	0.284	...	...	...	...	...
GJ 663 A	K1.0V	...	...	0.523	1.118	0.595	...	...	...	...	...
GJ 663 B	K1.0V	...	...	0.523	1.118	0.595	...	...	...	...	...
GJ 664 (C)*	K5.0V	0.581	4600	0.295	0.629	0.334	...	...	...	...	...
GJ 666 A	G8.0V	0.841	5200	0.545	1.164	0.619	...	...	...	...	...
GJ 667 A	K3.0V	...	...	0.399	0.853	0.454	...	...	...	...	...
GJ 667 B	K5.0V	...	...	0.285	0.607	0.322	...	...	...	...	...

Table 8—Continued

Name	SpType	Model					Model FixR				
		R ( $R/R_{\odot}$ )	$T_{\text{eff}}$ (K)	EHZ Inner R (AU)	EHZ Outer R (AU)	EHZ Lin (AU)	R ( $R/R_{\odot}$ )	$T_{\text{eff}}$ (K)	EHZ Inner R (AU)	EHZ Outer R (AU)	EHZ Lin (AU)
GJ 673	K7.0V	0.644	4100	0.259	0.554	0.295	...	...	...	...	...
GJ 702 A	K0.0V	0.754	5500	0.547	1.168	0.621	0.670	5700	0.522	1.114	0.593
GJ 702 B	K5.0V	0.411	5100	0.256	0.735	0.479	...	...	...	...	...
GJ 721	A0.0V	2.543	9800	5.852	12.50	6.648	...	...	...	...	...
GJ 764	K0.0V	0.694	5500	0.503	1.075	0.572	...	...	...	...	...
GJ 768	A7.0V	1.701	7800	2.480	5.297	2.817	...	...	...	...	...
GJ 783 A	K2.5V	0.751	5000	0.450	0.961	0.511	...	...	...	...	...
GJ 785	K2.0V	0.802	5100	0.450	1.068	0.618	...	...	...	...	...
GJ 827	F9.0V	0.970	6400	0.952	2.034	1.082	...	...	...	...	...
GJ 879 (B)*	K5.0V	0.592	4700	0.313	0.669	0.356	...	...	...	...	...
GJ 881 (A)	A4.0V	1.635	9200	3.316	7.084	3.768	...	...	...	...	...
GJ 884	K7.0V	0.553	4200	0.234	0.499	0.265	...	...	...	...	...
GJ 892	K3.0V	0.698	5000	0.418	0.893	0.475	0.778	4800	0.430	0.918	0.488

Note. — \* Designates wide component to above system with different GJ number.

This table shows model radius, temperature, inner and outer HZ radius, and the HZ width in AU in columns 3-7 for the extended 10 pc sample. HZs for GJ 663A, GJ 663B, GJ 667A, and GJ 667B are estimated using the  $V$ - $K$  relationship (see Section 5.2).

Table 9. Orbital Properties of Multiple Systems

Star	Sep	a	e	$i(^{\circ})$	$\Omega(^{\circ})$	$\omega(^{\circ})$	P(yr)	T	Ref
GJ 15 AB	40''	...	...	...	...	...	...	...	Eggen (1996)
GJ 34 AB	...	11''99	0.497	34.76	98.43	88.59	480	1889.6	Strand (1969)
GJ 53 AB	...	1''01	0.561	106.8	47.3	152.7	21.75	1975.74	Drummond et al. (1995)
GJ 65 AB	...	2''06	0.615	127.3	150.5	285.4	26.52	1971.88	Worley & Behall (1973)
GJ 66 AB	...	7''82	0.534	142.8	13.1	18.37	483.66	1813.5	van Albada (1957)
GJ 105 AC-B	165''	...	...	...	...	...	...	...	Golimowski et al. (2000)
GJ 105 AC	3''3	...	...	...	...	...	...	...	Golimowski et al. (2000)
GJ 166 A-BC	83''	...	...	...	...	...	...	...	Baize & Petit (1989)
GJ 166 BC	6''94	...	0.410	108.9	150.9	327.8	252.1	1849.6	Heintz (1974)
GJ 216 AB	95''	...	...	...	...	...	...	...	Eggen (1956)
GJ 222 AB	...	0''688	0.451	95.94	126.36	111.57	14.11	1999.9	Han & Gatewood (2002)
GJ 234 AB	...	1''04	0.371	51.8	30.7	223	16.12	1999.38	Ségransan et al. (2000)
GJ 244 AB	...	7''56	0.592	136.5	55.57	147.27	50.09	1894.13	Gatewood & Gatewood (1978)
GJ 250 AB	58''	...	...	...	...	...	...	...	Eggen (1956)
GJ 280 AB	...	4''496	0.365	31.9	284.8	88.8	40.38	1967.86	Irwin et al. (1992)
GJ 412 AB	28''	...	...	...	...	...	...	...	Gould (2003)
GJ 423 AC-BD	...	2''533	0.421	112.1	101.3	127.3	59.84	1995.05	Heintz (1996)
GJ 423 AC	...	0''056	0.53	94.9	263.5	143.0	1.832	1986.50	Mason et al. (1995)
GJ 423 BD	*274,000km	...	...	...	...	...	0.015	...	Mason et al. (1995)
GJ 432 AB	17''	...	...	...	...	...	...	...	Henry et al. (2002)
GJ 442 AB	25''4	...	...	...	...	...	...	...	Poveda et al. (1994)
GJ 473 AB	...	0''926	0.295	103.00	143.48	347.2	15.64	1992.30	Torres et al. (1999)
GJ 559 AB	...	17''57	0.518	79.2	204.85	231.65	79.91	1875.66	Pourbaix et al. (2002)
GJ 551-GJ 559 AB	2°18	...	...	...	...	...	...	...	Poveda et al. (1994)
GJ 566 AB	...	4''94	0.51	139	347	203	151.6	1909.3	Söderhjelm (1999)
GJ 570 A-BC	...	32''34	0.20	72.53	317.31	252.1	2130	1689	Hale (1994)
GJ 570 BC	...	0''151	0.756	107.6	195.9	127.56	0.846	1996.51	Forveille et al. (1999)
GJ 570 ABC-D	258''3	...	...	...	...	...	...	...	Burgasser et al. (2000)
GJ 663 AB	...	13''0	0.916	99.79	-85.8	-90.2	470.9	1677.9	Irwin et al. (1996)
GJ 663 AB-GJ 664	74''2	...	...	...	...	...	...	...	Luyten (1957)
GJ 666 AB	...	10''42	0.779	35.64	131.78	333.44	693.24	1907.2	Wieth-Knudsen (1957)
GJ 667 AB	...	1''81	0.58	128	313	247	42.15	1975.9	Söderhjelm (1999)
GJ 695 AD	1''43	...	0.32	68.0	81.8	92	65	1951.0	Turner et al. (2001); Heintz (1994)
GJ 695 AD-BC	34''	...	...	...	...	...	...	...	Raghavan et al. (2010)
GJ 695 BC	...	1''36	0.178	66.2	60.7	174.0	43.2	1965.4	Couteau (1959)
GJ 702 AB	...	4''55	0.499	121.16	302.12	14.0	88.38	1895.94	Pourbaix (2000)
GJ 713 AB	...	0''124	0.428	74.42	230.30	119.3	0.768	1984.83	Farrington et al. (2010)
GJ 725 AB	...	13''88	0.53	66.0	136.9	234.6	408	1775.0	Heintz (1987)
GJ 783 AB	7''1	...	...	...	...	...	...	...	Poveda et al. (1994)
GJ 820 AB	...	24''43	0.414	52.7	173.4	153.17	691.61	1689.14	Baize (1950)
GJ 845 A-BC	402''3	...	...	...	...	...	...	...	Scholz et al. (2003)
GJ 845 BC	0''732	...	...	...	...	...	...	...	McCaughrean et al. (2004)
GJ 860 AB	...	2''383	0.410	167.2	154.5	211.0	44.67	1970.22	Heintz (1986)
GJ 866 AC	...	~0''01	0.000	~117	...	...	...	1991.71	Delfosse et al. (1999)
GJ 866 AC-B	...	0''346	0.446	112	161.5	337.6	2.25	1997.53	Delfosse et al. (1999)
GJ 881-GJ 879	1°97	...	...	...	...	...	...	...	Poveda et al. (1994)



Table 9—Continued

Star	Sep	a	e	$i(^{\circ})$	$\Omega(^{\circ})$	$\omega(^{\circ})$	P(yr)	T	Ref
GJ 1245 AC-B	7''969	...	0.320	135.0	80.0	38.0	15.22	1983.1	Tokovinin (1997)
GJ 1245 AC	0''800	...	...	...	...	...	...	...	Tokovinin (1997)
SCR 1845-6357 AB	1''170	...	...	...	...	...	...	...	Biller et al. (2006)

Note. — \*asin(i)

Table 10. Total EHZ by Spectral Type.

SpType	5 pc Sample		Total 10 pc Sample	
	# of stars	EHZ AU	# of stars	EHZ AU
A	0(1)	...	3 (4)	13.2
F	0(1)	...	4 (6)	4.9
G	3	2.6	14 (21)	11.9
K	7	2.9	34 (35)	15.4
M	48(50)	3.3	384*(400)*	26.1*

Note. — The numbers used in the table reflect the number of stars in each sample for which the EHZ was calculated (and include the Sun). Photometrically unresolved binaries, evolved stars, and substellar objects for which EHZs were not calculated are excluded from these totals. \*The totals for the M type population to 10 pc are a factor of eight greater than the population within 5 pc, estimated via scaling by the volume ( $R^3$ ). Numbers in parentheses are totals including photometrically unresolved binaries and evolved stars.

Table 11. Exoplanets within Ten Parsecs

Star	Planet	Semimajor Axis (AU)	$e$	Ref	HZinner (AU)	HZouter (AU)
GJ 139	b	0.1207±0.0020	0.0	Pepe et al. (2011)	0.632	1.350
GJ 139	c	0.2036±0.0034	0.0	Pepe et al. (2011)	0.632	1.350
GJ 139	d	0.3499±0.0059	0.0	Pepe et al. (2011)	0.632	1.350
GJ 144	b	3.39±0.36	0.702±0.039	Benedict et al. (2006)	0.439	0.938
GJ 176	b	0.066	0	Forveille et al. (2009)	0.136	0.290
GJ 442 A	b	0.46±0.04	0.34±0.14	Tinney et al. (2011)	0.689	1.472
GJ 506	b	0.05±5.0e-6	0.12±0.11	Vogt et al. (2010a)	0.689	1.472
GJ 506	c	0.2175±0.0001	0.14±0.06	Vogt et al. (2010a)	0.719	1.537
GJ 506	d	0.476±0.001	0.35±0.09	Vogt et al. (2010a)	0.719	1.537
GJ 559 B	b*	0.04185±0.0003	0	Dumusque et al. (2012)	0.541	1.155
GJ 581	b	0.04	0	Mayor et al. (2009)	0.083	0.179
GJ 581	c	0.07	0.17±0.07	Mayor et al. (2009)	0.083	0.179
<b>GJ 581</b>	<b>d</b>	<b>0.22</b>	<b>0.38±0.09</b>	<b>Mayor et al. (2009)</b>	<b>0.083</b>	<b>0.179</b>
GJ 581	e	0.03	0	Mayor et al. (2009)	0.083	0.179
GJ 581	f*	0.758±0.015	...	Vogt et al. (2010b)	0.083	0.179
<b>GJ 581</b>	<b>g*</b>	<b>0.1460±1.4e-4</b>	...	<b>Vogt et al. (2010b)</b>	<b>0.083</b>	<b>0.179</b>
GJ 667 C	b	0.049	0.172±0.043	Anglada-Escudé et al. (2012)	0.096	0.205
<b>GJ 667 C</b>	<b>c</b>	<b>0.123±0.020</b>	<b>&lt; 0.27</b>	<b>Anglada-Escudé et al. (2012)</b>	<b>0.096</b>	<b>0.205</b>
GJ 674	b	0.039	0.20±0.02	Bonfils et al. (2007)	0.098	0.210
GJ 785	b	0.310±0.005	0.30±0.09	Howard et al. (2010)	0.500	1.068
GJ 832	b	3.4±0.4	0.12±0.11	Bailey et al. (2009)	0.131	0.280
GJ 849	b	2.35	0.06±0.09	Butler et al. (2006)	0.136	0.290
GJ 876	b	0.2083±2.0e-5	0.0292±1.5e-3	Rivera et al. (2010)	0.090	0.191
<b>GJ 876</b>	<b>c</b>	<b>0.1296±2.6e-5</b>	<b>0.2549±8.0e-4</b>	<b>Rivera et al. (2010)</b>	<b>0.090</b>	<b>0.191</b>
GJ 876	d	0.0208±1.5e-7	0.207±0.055	Rivera et al. (2010)	0.090	0.191
GJ 876	e	0.3443±0.0013	0.055±0.012	Rivera et al. (2010)	0.090	0.191
GJ 881	b	115	0.11	Kalas et al. (2008)	3.316	7.084

Note. — Bold rows indicate the planet is in the EHZ for at least part of its orbit. \* Planet detection controversial.